



## Vibration Isolation and Attenuation Mounts

Level 2 Design Report

March 3, 2017

|              |                      |               |
|--------------|----------------------|---------------|
| R.S. Maguire | P.H. Gaskell         | K. Blundy     |
| L.R. Miller  | G.A. Hall            | B.A.H. Jones  |
|              | M. Valladares-Hodder | E.O. Hollands |

## Executive Summary

Microphonic effects exist in Hi-Fi systems wherein mechanical vibrations are transformed into unwanted electrical signals, termed noise, that consequently reduce sound quality. Isofonics have designed footers of aluminium and steel upon which such systems are to be supported that aim to isolate and attenuate the signals responsible for this aforementioned noise.

Three footers are required per system, three being the minimum number of points of contact necessary to support a rigid mass, and are to be sold as a device comprising a contained magnetic damping mechanism with two optional additional pieces for mounting: a removable base with a large surface area for uneven surfaces such as carpets and a removable spike with a point contact for coupling to equipment. The main device, base and spike are to cost £1149.00, £66.00 and £49.00 respectively, placing Isofonics at the higher end of the existing market due to its unique feature of tunability and premium quality components embodying a design that is both innovative and effective.

The device may be altered manually by the user to support a range of different masses, a feature of customisability unique to Isofonics. This process may also be informed by a user friendly phone application. Additionally, within this design lies potential for product families of differing size, catering to an even wider audience, and applications within the field of optics, more specifically in the optimisation of microscopes.

## Nomenclature

AISI American Iron and Steel Institute

DFA Design For Assembly

DFM Design For Manufacture

EMF Electro-Motive Force

ISO International Standards Organisation

$F_d$  Vertical applied load exerted on each top piece.

$F_m$  Vertical magnetic reaction exerted on each top piece.

$N_1$  Core race reaction force.

$N_2$  Top cone reaction force.

$P$  Vertical preload.

$c$  System damping coefficient.

$k$  System stiffness.

$f_d$  System damped natural frequency in Hz.

$f_n$  System natural frequency in Hz.

$p_d$  Horizontal applied load exerted on each bearing.

$p_m$  Horizontal magnetic reaction exerted on each bearing.

$\alpha$  Top cone slope.

$\beta$  Preloading backstop slope.

$\zeta$  System damping factor.

$\mu$  Frictional coefficient.

$\omega_d$  System damped natural frequency in  $\text{rad s}^{-1}$ .

$\omega_n$  System natural frequency in  $\text{rad s}^{-1}$ .

$T$  Preloading torque.

$\mu$  Coefficient of friction.

$\delta u$  Separation between the magnets

$u$  Horizontal displacement of the bearing

- $u_1$  Displacement of free magnet from the centre
- $u_2$  Displacement of the fixed magnet from the centre
- $y$  Vertical displacement of equipment.

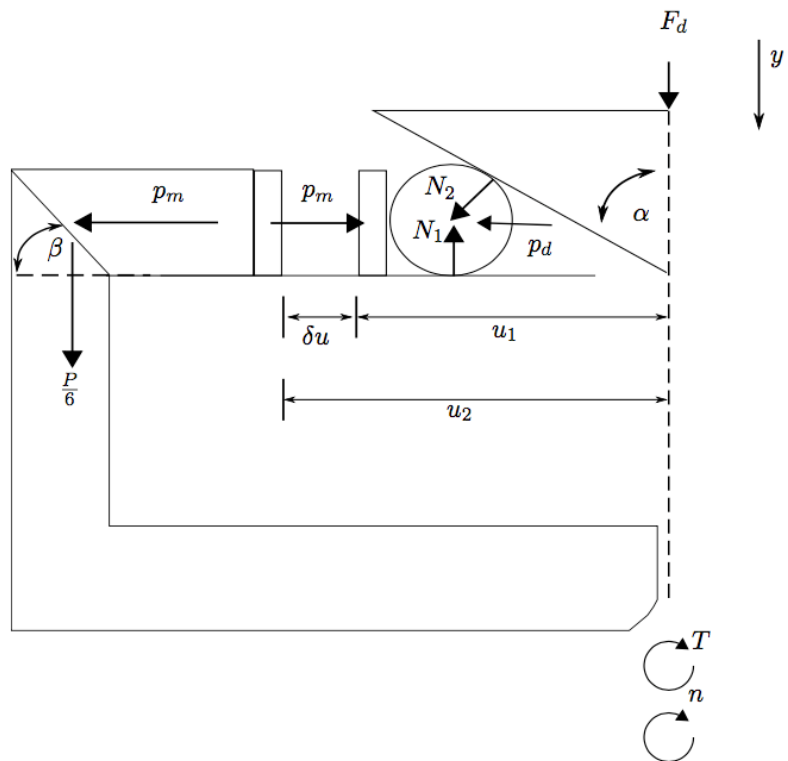


Figure 1: Nomenclature

## Contents

|          |  |           |
|----------|--|-----------|
| <b>1</b> | <b>Introduction</b> (GROUP 25)   | <b>1</b>  |
| <b>2</b> | <b>Design Concepts</b> (R.S. MAGUIRE)                                  | <b>2</b>  |
| 2.1      | Damping Mechanisms (R.S. MAGUIRE) . . . . .                            | 2         |
| 2.2      | Isolation Mechanisms (R.S. MAGUIRE) . . . . .                          | 3         |
| <b>3</b> | <b>Design Development</b> (R.S. MAGUIRE)                               | <b>8</b>  |
| 3.1      | Opposing Magnets (B.A.H. JONES, R.S. MAGUIRE) . . . . .                | 9         |
| 3.1.1    | Flux Path Simulation (G.A. HALL) . . . . .                             | 10        |
| 3.1.2    | Magnetic Stresses (G.A. HALL) . . . . .                                | 10        |
| 3.2      | Preloading Mechanism (B.A.H JONES, R.S. MAGUIRE) . . . . .             | 12        |
| 3.3      | Casing (B.A.H JONES, R.S. MAGUIRE) . . . . .                           | 12        |
| 3.4      | Materials (L.R. MILLER, R.S. MAGUIRE) . . . . .                        | 13        |
| 3.5      | Screw Specification (G.A. HALL) . . . . .                              | 14        |
| 3.6      | System Analysis (B.A.H. JONES) . . . . .                               | 17        |
| 3.6.1    | Parametric Model (B.A.H. JONES) . . . . .                              | 17        |
| 3.6.2    | System Tuning (B.A.H. JONES) . . . . .                                 | 24        |
| 3.6.3    | Experimentation (M. VALLADARES-HODDER) . . . . .                       | 27        |
| 3.6.4    | Dynamic Simulation (M. VALLADARES-HODDER) . . . . .                    | 30        |
| <b>4</b> | <b>Design for Manufacture</b> (E.O. HOLLANDS)                          | <b>33</b> |
| 4.1      | Bill of Materials (R.S. MAGUIRE) . . . . .                             | 34        |
| 4.2      | Finishes (E.O. HOLLANDS) . . . . .                                     | 36        |
| 4.3      | Manufacture Costs (E.O. HOLLANDS) . . . . .                            | 36        |
| 4.3.1    | Optimisation (E.O. HOLLANDS) . . . . .                                 | 36        |
| 4.3.2    | Costing (E.O. HOLLANDS) . . . . .                                      | 38        |
| <b>5</b> | <b>Design for Assembly</b> (E.O. HOLLANDS)                             | <b>38</b> |
| 5.1      | Jig Design (E.O. HOLLANDS) . . . . .                                   | 38        |
| 5.2      | Assembly Costs (E.O. HOLLANDS) . . . . .                               | 38        |
| <b>6</b> | <b>Design for Sustainability</b> (M. VALLADARES-HODDER)                | <b>39</b> |
| <b>7</b> | <b>Commercial Considerations</b> (L.R. MILLER, E.O. HOLLANDS)          | <b>40</b> |
| 7.1      | Brand Development and Competitor Analysis (L.R. MILLER) . . . . .      | 40        |
| 7.2      | Stillpoints Patent Check (L.R. MILLER, E.O. HOLLANDS) . . . . .        | 40        |
| 7.3      | Marginal Costs (E.O. HOLLANDS) . . . . .                               | 41        |
| <b>8</b> | <b>Discussion</b> (E.O. HOLLANDS)                                      | <b>42</b> |
| 8.1      | Specification Fulfilment (L.R. MILLER) . . . . .                       | 42        |
| 8.2      | Further Developments (L.R. MILLER, E.O. HOLLANDS, G.A. HALL) . . . . . | 43        |
| <b>9</b> | <b>Conclusion</b> (GROUP 25)   | <b>43</b> |

Vibration Isolation and Attenuation Mounts                          Group 25

|   |           |
|---|-----------|
| <b>A Project Plan</b> (M. VALLADARES-HODDER)  | <b>46</b> |
| <b>B Drawings</b> (G.A. HALL)                 | <b>48</b> |
| <b>C Assembly Instructions</b> (R.S. MAGUIRE) | <b>59</b> |

## 1 Introduction

Microphonics describes the phenomenon wherein internal components within an electronic device transform mechanical vibrations into undesired electrical signals [1]. In the context of hi-fi systems, and when these vibrations are within the frequency range audible to the human ear—20 Hz–20 kHz—they equate to noise that reduces audio quality and therefore threatens the user's listening experience. This report details the design of vibration isolation and attenuation mounts that minimise this interference as well as that originating from external sources.

The following function analysis tree defines the user requirement specification for the product:

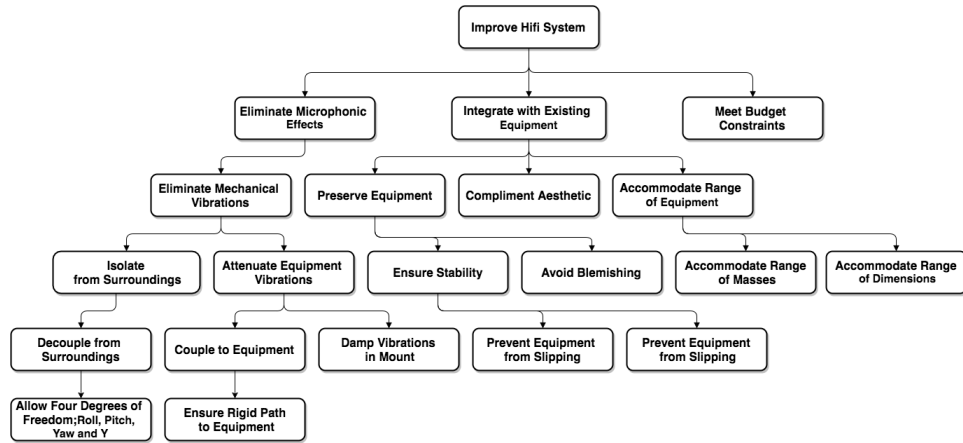


Figure 2: User Requirement Specification Diagram

With such a niche product consisting of high tolerance machined parts and premium materials comes a high cost, indicating a corresponding market; middle aged/mature clientele with strong technical understanding of the hobby and its principles or affluent younger hobbyists. The current market offers a range of mounts at a range of prices within which the product shall lie at the higher end, namely between £1 000–£1 500 per mount.

Market leaders such as Stillpoints<sup>®</sup>, Nordost<sup>®</sup> and Isoclear<sup>®</sup> offer sleek solutions yet lack the tailorability offered by our design, allowing customers to preload their mounts manually for individual amps, potentially with interactivity provided by an instructive technical app. After conducting market research via surveys, it was found that potential customers were very much interested in the ability to manually adjust their mount as appropriate and that this offered an invaluable, unique selling point.

This report covers the initial design concepts proposed by Group 25, the development of a chosen design, its design for manufacture and sustainability and its commercial considerations.

## 2 Design Concepts

During initial research it was noticed the most successful products on the market met three primary criteria:

- They allowed the mounted equipment to move with four degrees of freedom: three in translation and one in rotation.
- They used single degree of freedom systems for damping. Simpler damping mechanisms were more effective at consistently attenuating unwanted frequency components.
- Vibrations were efficiently transmitted to the damping system from the equipment. This was typically achieved using hard materials and limited contact between the footer and equipment.

In summary, any concepts generated had to first *isolate* the equipment then *attenuate* vibrations by allowing the equipment to move freely and then damp vibrations in controlled manner.

In order to simplify the process of concept generation, the formulation of isolation and attenuation mechanisms was separated. Isolation mechanisms were designed to translate the four degrees of freedom in the movement of the equipment into the single degree of freedom of the damping mechanism. Those single degree of freedom damping mechanisms were designed to be easily applied to multiple isolation concepts.

### 2.1 Damping Mechanisms

Three methods of damping were considered—not including the friction in bearings, which cannot be completely eliminated. These were viscoelastic, magnetic and fluid damping.

Viscoelastic materials, such as rubber or Sorbothane<sup>®</sup>, heat up when subjected to changes in mechanical stress [2]. Hence, the amplitude of vibrations are reduced when the driving oscillations are transmitted through viscoelastic materials. Typically when these materials are used in footers, the vibrations are not limited to a single degree of freedom, so the effectiveness of attenuation depends on the vibration direction. This makes it difficult to model and specify a single system natural frequency or damping factor.

Figure 3 on the following page details how viscoelastic materials can be used in a system where vibrations have been translated to a single direction. A linear bearing compresses a viscoelastic sleeve on the same shaft.

Magnets can also be used to damp vibrations when constrained to a single direction. As a permanent magnet travels through a coil, an EMF is induced due to Faraday's law, which drives a current when the circuit is complete. The current flowing generates a magnetic field opposing the

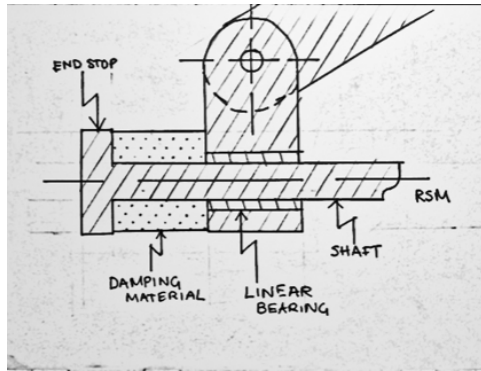


Figure 3: D1—Viscoelastic damping mechanism.

permanent magnet, according to Lenz's law. A possible assembly for this system is detailed in Figure 4. The strength of magnets were to be tuned to the desired dynamic properties of the system.

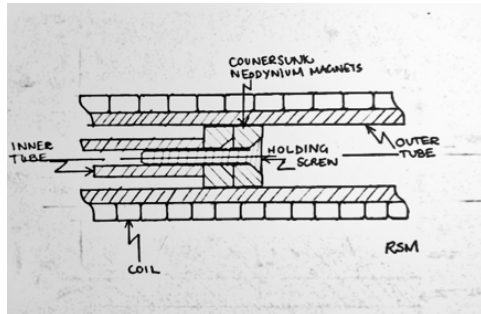


Figure 4: D2—Magnetic damping mechanism.

Finally, a simple fluid damping system was considered, whereupon a bearing travels through some viscous fluid. Skin friction provides the damping force in Figure 5 on the following page. The size of the bearing could be tuned to meet the required constraints for damping factor and natural frequency. However, this concept was difficult to realise in any manufacturable assembly whilst successfully containing the fluid.

## 2.2 Isolation Mechanisms

Early concepts made use of linkages to transform vertical and lateral oscillations into lateral oscillations along damped linear bearings, which would have been most easily realised using a viscoelastic damper. Figure 6 on the next page details one such embodiment.

Some components of vertical vibrations were not damped by the mechanism in Figure 6; these were transmitted to the base of the mount such that the mount was not completely isolated. Repeating the mechanism by using

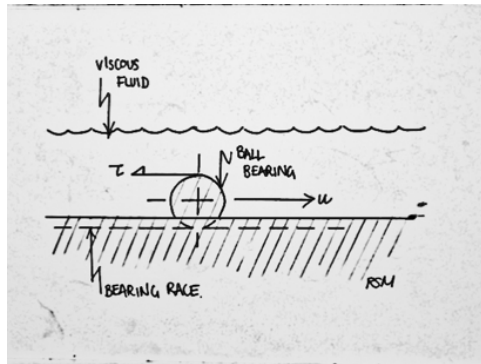


Figure 5: D3—Fluidic damping mechanism.

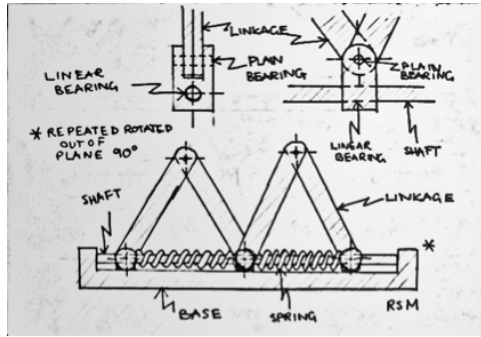


Figure 6: C1—Simple linkage mechanism.

multiple layers of linkages was explored in the concept detailed in Figure 7 on the following page. Each layer damps a fraction of the vertical oscillations transmitted downwards by the layer above resulting in more isolation.

However, the fundamental issue with linkage based isolator mechanisms is the feature size of those linkages. Thin members are prone to resonance with large amplitudes at relatively lower frequencies, possibly within the audible spectra (20 Hz–20 kHz).

Spherical bearings also featured in design concepts. Figure 8 on the next page describes one such embodiment where a layer of spherical bearings were sandwiched between two platforms. The upper platform was to be made of a hard material such as stainless steel or tungsten carbide, in order to efficiently transmit vibrations through to the bearings via point contacts. The bearings allowed the top platform to move with the equipment in three degrees of freedom: two lateral directions and lateral rotation. The bottom platform would have been made of some viscoelastic material with holes for the bearings to rest in. Both vertical and lateral oscillations would have been damped by this platform and dissipated as heat.

This concept had a major drawback: the damping mechanism was not confined to a single degree of freedom. It would have been challenging to

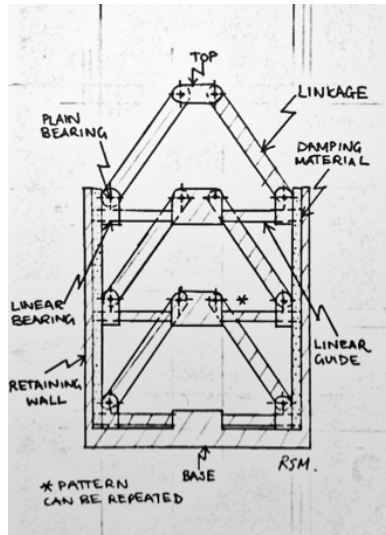


Figure 7: C2—Layered linkage mechanism.

determine a single damping factor and resonant frequency. The isolation mechanism was an anomaly in the concept generation phase, as the damping mechanism was not interchangeable with those in Section 2.1 on page 2.

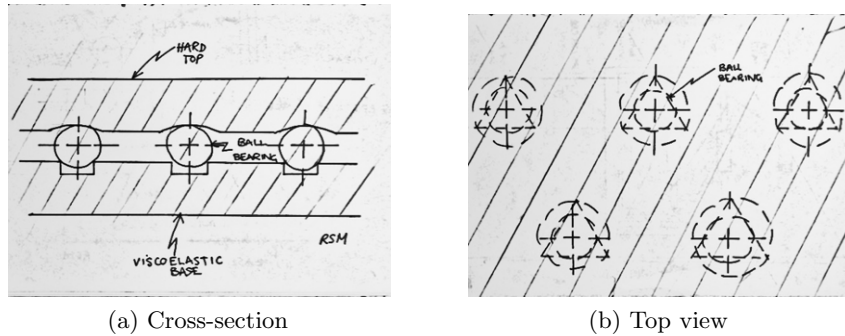


Figure 8: C3—Viscoelastic platform concept.

Isolation cones are a popular type of mount, an example is Nordost's Sort Kones®. The Sort Kones are made of three parts: a post, spherical bearing, and cone. The bearing rests on the top of the post and the cone sits on top of the bearing, such that the cone is free to swivel and rotate. However, cones seek only to isolate the mounted equipment and allow free movement—they do not attenuate vibrations.

Figure 9 on the next page demonstrates how an attenuating mechanism could have been incorporated into the post of an isolation cone. The spring in the isolation mechanism could have been replaced with one of the damping mechanisms in Figure 3 and Figure 4.

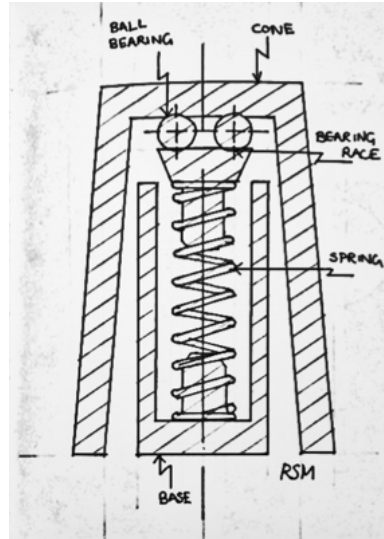


Figure 9: C4—Damped cone concept.

An alternative mechanism was devised to translate horizontal and lateral oscillations into oscillations of a spherical bearing along a race. Figure 10 on the following page details the geometry required to achieve this translation.

When no force is applied to the top piece, the bearing would travel to the bottom of its race. Increasing the load would cause the bearing to move up the race due to the gradient of the curve on the top piece, which was greater than the gradient of the race. There would be some component of the reaction force acting on the bearing perpendicular to the curve which points up the slope of the race. However, the gradient of the curve decreases travelling up the slope, so for a given load the component of the reaction force would also decrease. Therefore, for each load, there is a different equilibrium position somewhere along that race where the components of the bearing's weight and the reaction force acting on the bearing in the direction of the race are equal and opposite. The mechanism acts as a geometric spring with some stiffness.

The frictional shear forces in the mechanism would provide significant damping due to the magnitude of the reaction forces involved. Furthermore, one of the damping mechanisms in Figure 3 or Figure 4 could be coupled to the linear motion of the bearings to tune the system to a desired natural frequency and damping factor—this could result in quite a large footer.

A drawback of this concept is difficulty in containing the bearings, the user would be free to remove the top piece, and the bearings would all come out of their races. Competitors could easily see how the mechanism works and replicate it for themselves.

Figure 11 on page 8 details a variation of C5, whereby the bearings travel outwards up the slope. This creates more space for a damping mechanism

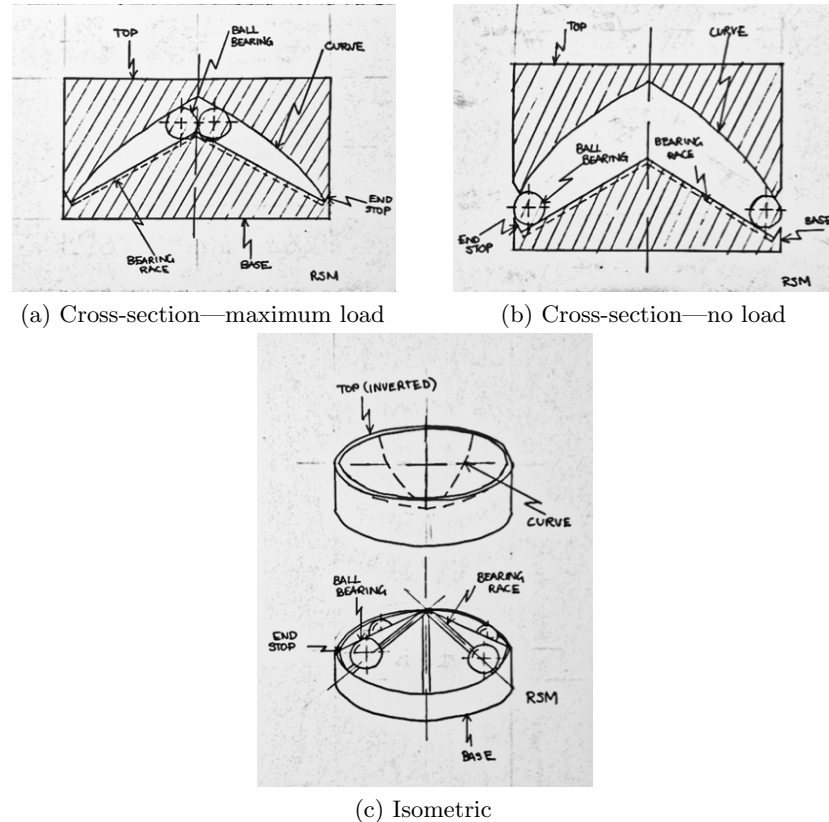


Figure 10: C5—Cone and bearing concept.

for each race around the outside of the footer. A fluid could be contained in the cavity in the bottom piece to damp vibrations using the mechanism described in Figure 5.

The flexibility of the alternative cone and bearing concept C6, coupled with its innovative design set the concept apart from its alternatives. In [3], it was shown how concept C6 with damping mechanism D2 best matched the customer's expectations and engineering requirements. This is the concept which informed the next stage of development and our final design.

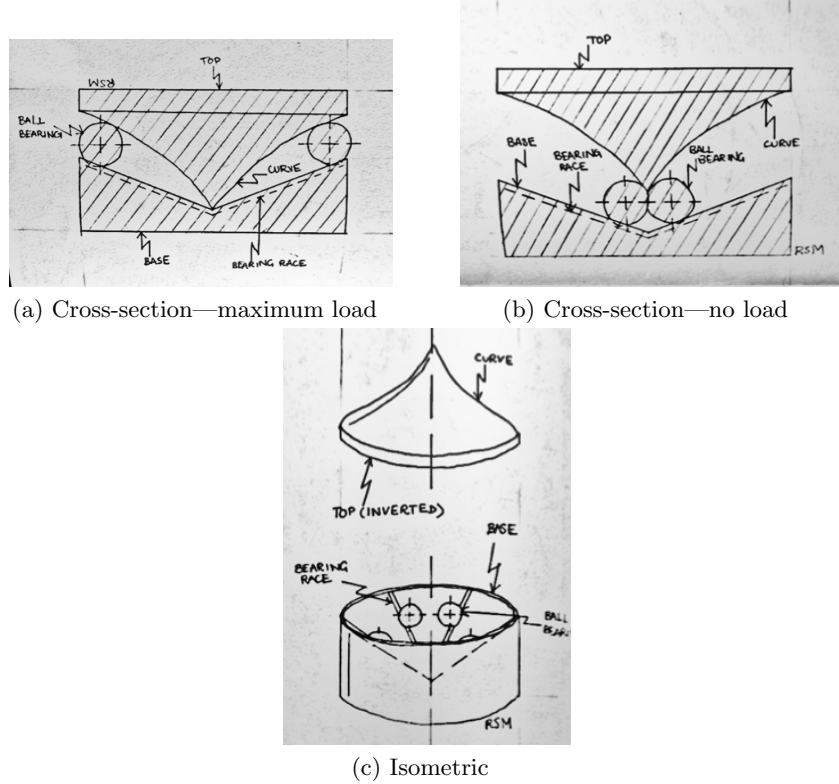


Figure 11: C6—Alternative cone and bearing concept.

### 3 Design Development

Through an iterative process, the concept highlighted in [3] for its promise was increasingly refined to produce a final design. The key milestones in development are as follows:

- The transition from curved geometry to opposing pairs of rare earth magnets to support the equipment's weight.
- The addition of a user-adjustable preloading mechanism to increase the range of masses that could be supported to full mass range of amplifiers: 5 kg–30 kg [3].
- The casing required to contain the isolation mechanism and dissuade the user from dismantling the footers.
- The choice of materials used for various parts in the system.
- The development of the models used to tune the design to meet performance requirements.

### 3.1 Opposing Magnets

Early in the development process, it became apparent the curved geometry of concept C6 in Figure 11 would not be able to support a particularly wide range of masses. Initially, a ring magnet mounted on the end of a rod was to be coupled to the bearings to damp oscillations, biased using a compression spring—see Figure 4.

To simplify the design and increase the supported mass range, the inclined bearing races in the base and curve in top piece were removed, and replaced with flat bearing races and a cone respectively. The damping mechanism was replaced with six pairs of opposing rare earth button magnets, with the opposing poles of magnets in adjacent races changing from N–N to S–S to N–N etc. The direction of poles alternate to allow the flux to flow in closed loops, and avoid flux leakage out of the system. Hysteresis losses in the base piece and frictional forces provide the damping forces in this system.

Figure 12 on the following page shows how the magnets and bearings would be arranged in a mount with opposing magnet pairs. These drawings have six races for a multitude of reasons:

- The number of opposing pairs had to be an even number to allow the poles of magnets in adjacent races to point in alternating directions for *all* races. Otherwise the behaviour of the repulsive forces in some races would be different to the others.
- At least four races were required to allow freedom of movement in both lateral directions.
- Using more races would require a larger diameter for the same usable travel distance.
- Finally, because the magnetic repulsion force is not a linear function of separation distance, oscillations parallel with a race would experience a greater stiffness than those between races. Mounts with more races would have less variation in lateral stiffness in different lateral directions.

The choice of six races was a compromise between the size of the mount and having a mount with a more constant stiffness in different lateral directions.

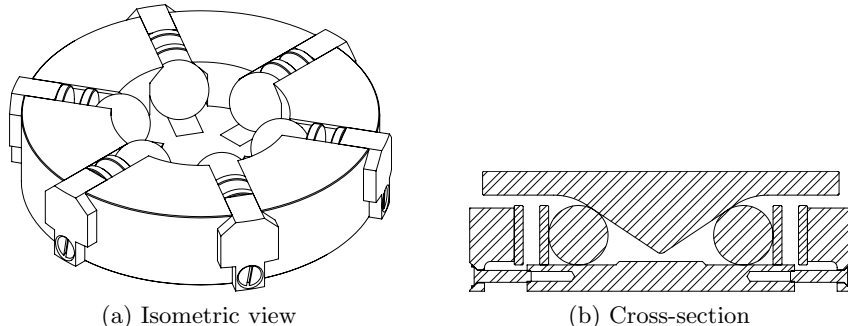


Figure 12: Isometric view and cross-section of initial design revision.

### 3.1.1 Flux Path Simulation

As the footer houses twelve rare earth magnets, considerations had to be made for the way in which these magnets interact with the surroundings of the footer as they could cause damage or interfere with mounted or surrounding equipment footer. Using a software package called MagNet® produced by infolytica®, it was possible to perform a 2D finite element analysis of the footers, allowing the effects of these magnets to be modelled. The analysis performed in this section is for the geometry of the final design, but the same procedure was performed following each significant revision during the design process. When modelling the effect of these magnets the two extreme cases were considered: at minimum and maximum separation as detailed in Figure 13.

It can be seen that the flux density outside of the footer is negligible as it has a value of the order  $10^{-5}$  T meaning that there would be minimal to no interactions between the footer and its surroundings as nearly all of the magnetic flux is contained within the core of the device.

### 3.1.2 Magnetic Stresses

The opposing pole pairs of magnets housed within the core of the design exist in a highly stressed state, meaning that the force applied to each magnet is large and has to be considered. The maximum force acting between the magnets is  $p_{m\max}$  and from this the maximum stress within the magnet could be calculated. This was shown to be 0.175 MPa. Reference [4] gave the yield stress for a neodymium magnet as 3.96 MPa meaning that there is a factor of safety of 23 per magnet. This suggests these magnets will not structurally fail during the operation of this product.

Again this analysis was performed on the final design revision, but similar analysis was performed at multiple stages during the design development process.

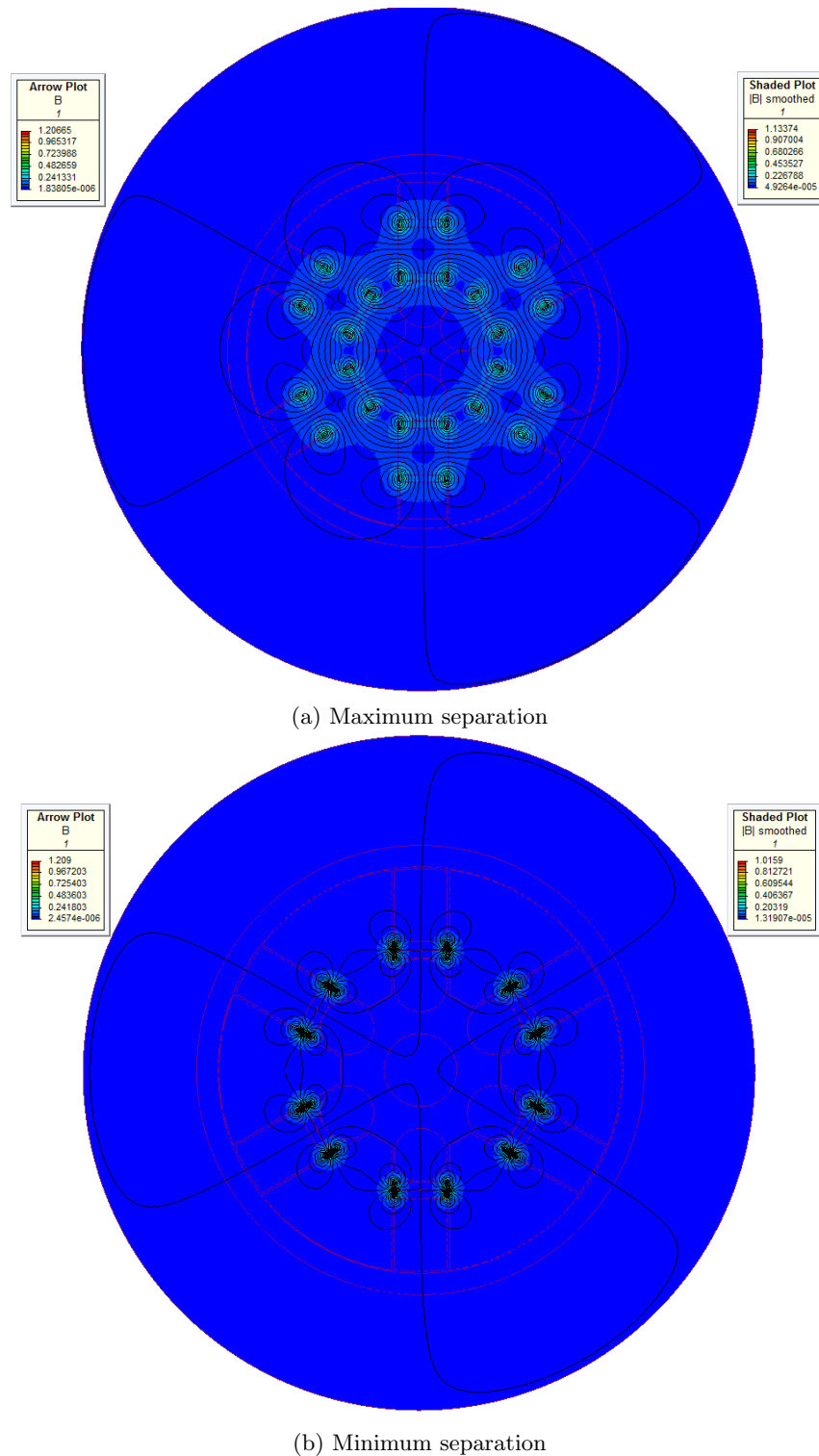


Figure 13: Flux density due to opposing magnets.

### 3.2 Preloading Mechanisms

Reference [3] identified the opportunity in the market for a footer that the user could tweak to their system. A preloading mechanism was included which changed the range of masses that could be supported by altering the position of outermost ring of magnets.

Figure 12 on page 10 contained a preloading system which the user tweaked by adjusting six screws—one for each bearing race. Tightening the screws moved the backstop part positioned behind the outermost magnet inwards.

A major issue with this initial design was that in order to preload the mechanism, all six individual backstop needed to be adjusted individually, proving incredibly tedious for the customer. Figure 14 details the geometry of the preloading crown. The crown slotted into the core of the footer through which the bearing races ran. The backstops contained a slope which matched the slope on the tips of the crown.

Also visible in the cross-section in Figure 14 is a hole through the centre of the crown and core piece. By threading the hole through the centre of the core, a single preloading screw was used to adjust the height of the crown relative to the rails. As the crown moved up, the backstops were pushed in. Only one screw was required to set a preload position for every rail.

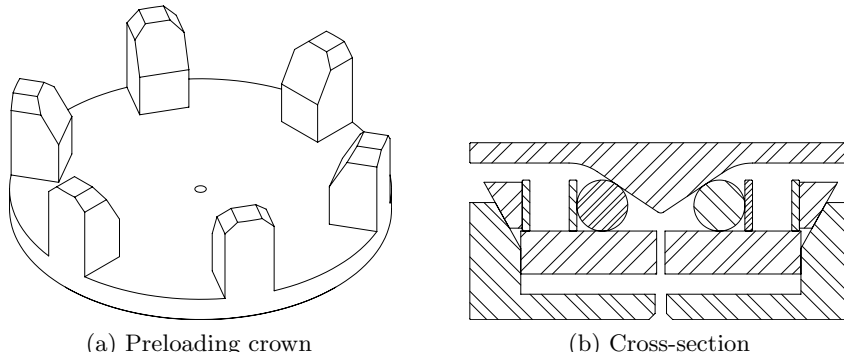


Figure 14: Design revision with revised preloading mechanism.

### 3.3 Casing

A problem with the design so far was that the top piece was not restrained. This means that if no load was applied, the force exerted by the magnets would push the top off and internal components would fall out of the core. A 4 mm retainer wall component was therefore designed. This was essentially a tube that fitted over the core and top piece which it then retained using an internal flange; this can be seen in Figure 15 on the next page. Six screws fastened the retainer to the core of the footer. In this revision the preload

crown and core thickness were adjusted to enable the full range of travel for the backstop without the preload screw going all the way through the core.

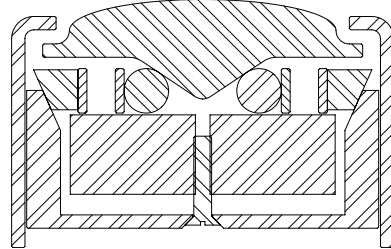


Figure 15: Design revision with retainer.

However, the casing also had to dissuade the user from disassembling the footer. It would not be desirable for competitors to easily reverse engineer the mechanism. A threaded insert was created for the bottom piece with a hole for accessing the preloading screw. The hole was designed to be smaller than the head of the screw so it could not be fully removed along with the preloading crown. The hole doubled as a mounting thread.

The threaded insert was designed to be some ISO metric standard. An M80 x 4.0 thread was chosen as it was close to the size of existing footers on the market. The required drill hole size for M80 x 4.0 threads is  $\phi 76$  mm. This worked well with a  $\phi 10$  mm bearing and ring magnet—the magnet pairs just touched at maximum load and preload.

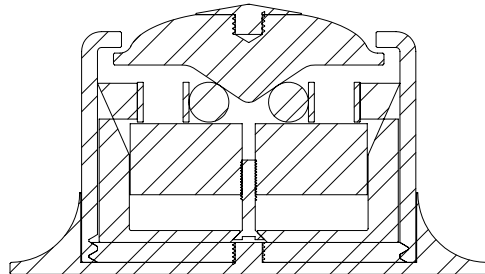


Figure 16: Final design with threaded base and attachments.

### 3.4 Materials

Neodymium magnets are the most widely used type of rare-earth magnet, strongest type of permanent magnet commercially available and of greatest benefit in applications where there is limited space—such as for the opposing magnet pairs in these footers.

Tungsten carbide possesses a Young's modulus of 530 GPa [5], more than two times of that of AISI 316 stainless steel [6]; a material commonly used for spherical bearings. Due to Hooke's law, the material does not undergo large

deflections which in turn ensures efficient energy transfer between the Hi-Fi components. The bearings do not require any lubrication as they grind down any particulates that may enter the system. Tungsten carbide was selected for the bearings in this project.

With regards to the custom machined parts, there are two options: AISI 304 stainless steel and 6061-T6 *aircraft-grade* aluminium. Stainless steel is harder so, in a similar way to tungsten carbide, is a more efficient transmitter of vibrations. It is also harder wearing so more suitable for moving parts. Aluminium, being softer [7], is cheaper to cut. A part machined in stainless steel will cost around 30% more than the same part machined in aluminium<sup>1</sup>, given there are no delicately thin features which would benefit from the stronger material.

Considering this, the aluminium alloy was selected for the purely structural parts, leaving 304 stainless steel for the core part (COR080-0003) which the bearings are contained in and flux must be able to travel through; the top piece (TOP080-0004) which pushes the bearings along the race; and the user replaceable spike (USR080-0001) which the vibrations are conducted through.

### 3.5 Screw Specification

The design features seven screws, six of which are to be used to attach the retaining wall to the core, with the other being used as a means of preloading the system. All of these screws are to be made of A2 tool steel which has a yield stress,  $\sigma_y$ , of 205 MPa in tension [8] and therefore through the Von Mises yield criterion it is possible to achieve its yield stress in shear. The yield criterion is as follows:

$$k = \frac{\sigma_y}{\sqrt{3}} \quad (1)$$

where  $k$  is the stress at failure. For A2 tool steel this value was 118 MPa.

Due to the nature of the retaining wall used to constrain the preloading backstops in their tracks, there is a shear force applied to the six retaining wall screws. At the worst possible instance the shearing force on one of these screws was a sixth of the total weight resting on the footer. It was decided that a single footer should not structurally fail in the event of a person accidentally stepping on it, meaning that these six retaining wall screws were specified to withstand the weight of a 140 kg mass between them.

Reference [9] recommends preloading the screw to twice of the applied load in order to increase the friction between the core and the screw and increase the screw's resistance to loosening. Hence, the total load applied to the screw is the sum of the preload and the applied load—this equates to 700 N.

---

<sup>1</sup>Sylatech Ltd.

The stress analysis was performed on the screws to find what diameter would be required such that the screws could meet this specification. The screws' interaction with the core piece allowed for them to be modelled as a cantilever with a uniformly distributed load across its top edge as can be seen in Figure 17. Using this model the maximum shear stress within the screw was considered for various diameters of ISO metric threads, the results of the analysis can be seen in Table 1.

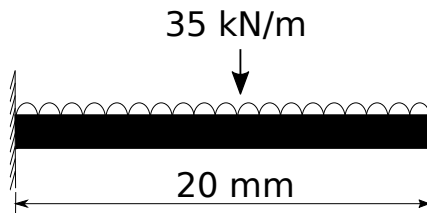


Figure 17: Retainer screw.

Table 1: Stress concentration analysis of the retainer screws.

| Thread | D / mm | $\tau$ / MPa | Suitable |
|--------|--------|--------------|----------|
| M1.6   | 1.25   | 586.8        | No       |
| M2     | 1.60   | 358.1        | No       |
| M2.5   | 2.05   | 218.1        | No       |
| M3     | 2.50   | 146.7        | No       |
| M3.5   | 2.90   | 109.0        | Yes      |
| M4     | 3.30   | 84.2         | Yes      |

When considering the preloading screw at the bottom of the footer, the load was applied along its top edge, so it was modelled as a strut with a single point load on top. Again, the worst possible case of applied load to the screw was the full 140 kg mass being supported by it as may be seen in Figure 18 on the following page. Therefore, the maximum stress case within the screw was considered for this applied load and tested for various diameters of ISO metric threads, as can be seen in Table 2 on the next page.

As can be seen from Table 1 and Table 2, for both cases an M4 thread screw meets the specification and therefore shall be used in the design. By specifying the screws for a 140kg mass per piece, there has been a large factor of safety considered for the pieces as the maximum mass which the design has been specified to work for is a 44.6kg mass supported by three footers meaning that the screws have a factor of safety of at least 9.4.

The final design contained a preloading mechanism which relied upon the user being able to operate the preloading screw. To ensure that the torque

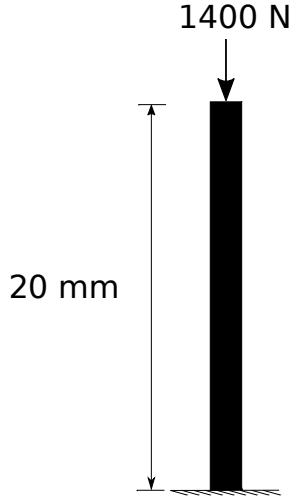


Figure 18: Preload-screw.

Table 2: Stress concentration analysis of the preload screw

| Thread | D / mm | $\sigma$ / MPa | Suitable |
|--------|--------|----------------|----------|
| M1.6   | 1.25   | 1140.0         | No       |
| M2     | 1.60   | 696.3          | No       |
| M2.5   | 2.05   | 424.4          | No       |
| M3     | 2.50   | 285.2          | No       |
| M3.5   | 2.90   | 212.0          | No       |
| M4     | 3.30   | 163.7          | Yes      |
| M5     | 4.20   | 101.1          | Yes      |
| M6     | 5.00   | 71.3           | Yes      |

required to operate this screw was within human capabilities a static analysis was performed. The factors which effect the torque required to preload the system are: the coefficient of friction  $\mu$  between the screw and its mating thread; the nominal bold diameter  $D$  and the bolt tension  $P$ . The required torque  $T$  is given by the following:

$$T = \mu DP \quad (2)$$

For stainless steel,  $\mu$  is 0.8 [10] and for the M4 screw,  $D$  is 4 mm. From Figure 1 it can be seen that there is a force  $p_m$  applied horizontally through the preloading backstop that causes a resultant force  $P/6$  acting on each of the six vertical struts of the crown. These forces were resolved find  $P/6$ :

$$\frac{P}{6} = p_m \tan(\beta) \quad (3)$$

where  $\tan(\beta)$  was 2.25.

To preload the system, the user has to remove all load from the footer, so the bearings will rest at a maximum distance away from the backstop. The magnetic repulsion force  $p_m$  reaches a maximum when the magnet separation is at a minimum—at maximum preload. This value  $p_{m\max}$  was 1.23 N. Equation 3 was substituted into Equation 2:

$$T_{\max} = 6 \mu D p_{m\max} \tan(\beta) \quad (4)$$

which yielded a  $T_{\max}$  value of 0.053 Nm, well within human capabilities given [11] quotes the 5th percentile for the maximum torque applied due to wrist pronation as 7.21 Nm.

### 3.6 System Analysis

As denoted by the user requirements specification tree in the feasibility report, the footer must be able to support a sufficiently large range of masses with dynamic properties spanning across a suitable interval. For example, the natural frequency and damping factor what magnets and dimensions need to be chosen. Once determined using the parametric model, these parameters were inputted into a computational simulation of the footer's behaviour, entailing the driving force (audio from Hi-Fi) and the additional damping caused by the repulsion between the magnets. As such this would provide proof of concept and provide related coefficients for different types of loading and material.

#### 3.6.1 Parametric Model

##### Preload System

Since the preload screw is what the user changes, it is the independent variable. Before considering how the preload affected the system, the method of preloading was analysed. To preload the system, the preload screw must be tightened with its rotational movement converted into vertical movement. The relationship is determined by the pitch of the thread on the screw and outlined below:

$$y = P n \quad (5)$$

where  $y$  is the vertical movement of the screw and therefore the crown,  $P$  is the pitch of the thread, and  $n$  is the number of revolutions. Next, the vertical movement of the crown must be translated into the radial displacement of the back stops. Since each rail is independent but identical, they can be considered from a perspective of a 2D cross section. The radial displacement can therefore be considered as a horizontal motion along the rail. By considering trigonometry and accounting for the mount's tolerances, the horizontal displacement can be written as:

$$x = \frac{y}{\tan(\beta)} \quad (6)$$

where  $x$  is the distance a back stop travels along its rail.

### Modelling Forces and Masses

For any particular preload, a range of masses must be placed on the footer before either of the extreme cases occur (bottom out and top out). If the system is considered to be in a steady state, the repulsive forces due to the magnets are balanced by the horizontal force on the bearings due to the resting mounted mass. Using Gilbert's model, the repulsion force [12] exerted by two identical opposing cylindrical magnets lying upon a common axis can be approximated by:

$$p_m = \frac{\pi \mu_0 M^2 r^4}{4} \left( \frac{1}{\delta u} + \frac{1}{(\delta u + 2t)^2} - \frac{2}{(\delta u + t)^2} \right) \quad (7)$$

Where  $r$  is the radius of the cylindrical magnet,  $\mu_0$  is the permeability of free space,  $M$  is the magnetisation of the magnets, and  $\delta u$  is the separation between magnet surfaces. To solve this equation, some parameters must be known. Firstly, the resting distance between magnets can be found by considering the dimensions of the rail:

$$\delta u = u_2 - u_1 \quad (8)$$

The magnetisation of the magnets is the second unknown in Equation 7. With the orientation of magnets in mind, this is given by:

$$B_0 = \mu_0 M \quad (9)$$

Where  $B_0$  is the flux density very close to the magnet surface. However, magnet strength is commonly rated using magnetic pull. This can be converted into flux density using [13].

$$B_0 = \sqrt{\frac{2 \text{pull} g \mu_0}{A}} \quad (10)$$

Where  $\text{pull}$  is magnetic pull in kg,  $g$  is the acceleration due to gravity, and  $A$  is the area of the surface being considered. So now for any particular magnet strength and dimensions, as well as magnet separation, the repulsion force can be determined. Since the system is being considered in a steady state the magnetic repulsion must be equal to the horizontal force component on a single bearing due to a mounted mass. These forces can be equated after considering the bearing-top piece integration angle  $\alpha$ .

$$F_d = \frac{p_d}{\cos(\alpha)} \quad (11)$$

With three footers being used, there are eighteen sets of magnets providing a repulsive force. So to find the mass that could rest for any specified pre-load, the net sum of the forces must be taken from all the magnet pairs:

$$F_d = \frac{18 F_d}{9.81} - 0.266 \quad (12)$$

where the *mass* is the mass resting on three feet. Note that the mass of the top piece although small is not negligible, so it must be subtracted from the calculated mass.

As described, for each preload value, there exists a different range of masses that could be supported. The interval can be determined by how low the top piece sits on the bearings. In turn this affects the distance from the centre of the core to the outer surface of the inner magnet. A clearance of 2 mm was given at each extreme to account for the real system's oscillations. With these boundary conditions, an envelope representing the range of supported masses was plotted—see Figure 19. Note that this plot was produced using the initial dimensions for the footer where:  $D_b = 76$  mm,  $D_s = 10$  mm,  $t = 2$  mm,  $r = 2$  mm,  $pull = 1.23$  mm preload.

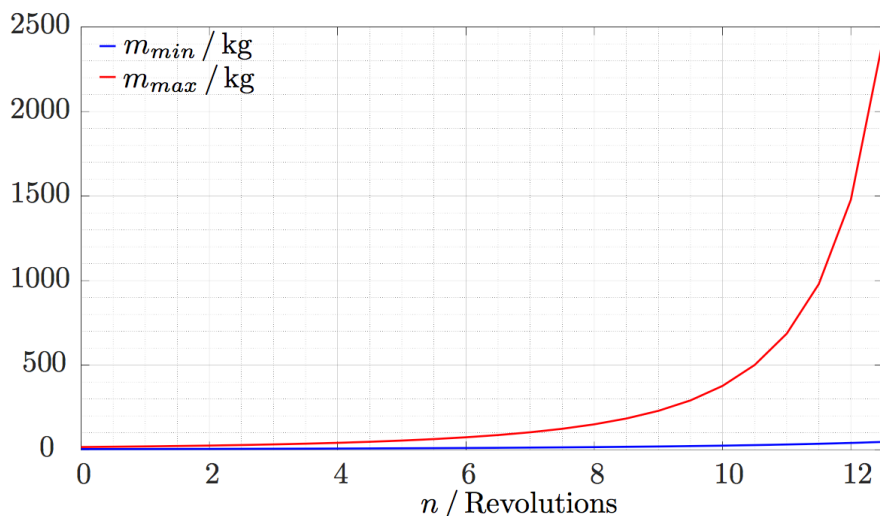


Figure 19: Graph of preload vs the maximum and minimum supported mass on three footers.

### Modelling Damped Natural Frequency

Another incredibly important factor that had to be considered was the damped natural frequency of the system. If the damped natural frequency of the system is too high or low, then the footer could interfere adversely with the mounted equipment. Within Hi-Fi equipment some of the lowest notes are as small as 20 Hz. Frequencies below 6 Hz can begin to cause an effect called rumble caused by excitations such as footsteps where they adversely affect the system. These two conditions provide boundary conditions for our

system, and suggest that if the footer has a damped natural frequency of between 6Hz and 20Hz it will have minimal effect on device resting upon it.

To further ensure that a mounted device was unaffected, it was decided to constrain the system's damped natural frequencies range even further. To do this a neighbouring technology was considered, that being tonearms on record players. Tonearms are another high quality, no expense spared industry. They face a similar problem of needing to limit the damped natural frequency of their system to minimise any effect on the turntable and hi-fi equipment. In the tonearm industry it is very common to have systems with resonance frequencies of 8 Hz–12 Hz [14]. This range was to be matched in the isolation and attenuation mount.

Initially it was thought that the stiffness of the system with three footers could be determined using Hooke's Law:

$$F = k e \quad (13)$$

Where  $F$  is the force due to stiffness,  $k$  is the stiffness and  $e$  is the spring or material extension. However, the force exerted by the magnets is nonlinear and so Hooke's Law cannot provide an accurate depiction of the footer. As a result a first order differential equation was used to an equivalent stiffness for each extension:

$$\frac{dF}{de} = k \quad (14)$$

From here, the natural frequency, both undamped and damped, of the system was found from the previous calculations of the resting mass and stiffness:

$$\omega_n = 18 \sqrt{\frac{k}{mass}} \quad (15)$$

$$\omega_d = \omega_n \sqrt{1 - \zeta^2} \quad (16)$$

Where  $\omega_n$  is the system natural frequency in radians per second,  $\omega_d$  is the system's damped natural frequency, and  $\zeta$  is the damping factor of the system. The damping factor is not constant however and it needs to be calculated for each specific natural frequency:

$$\zeta = \frac{c}{2 mass \omega_n} \quad (17)$$

where  $c$  is the damping coefficient of the system. This damping coefficient is a physical property and is found by considering energy losses. To determine it accurately it would need to be found empirically by performing experiments on prototype devices. However, it was possible to make a rudimentary evaluation of the problem to estimate a value for the damping coefficient.

First consider the definition of frictional forces:

$$\text{frictional force} = \mu N \quad (18)$$

Where  $\mu$  is the coefficient of friction between the two surfaces and  $N$  is the force normal to the point of contact between surfaces. Then consider definition of damping forces:

$$\text{damping forces} = c_{node} \dot{u} \quad (19)$$

Where  $\dot{u}$  is the velocity of the moving part and  $c_{node}$  is the damping coefficient at the point of contact being considered. Now by equating equations 18 and 19 a relationship between the damping coefficient and the coefficient of friction can be developed:

$$c_{node} = \frac{\mu N}{\dot{u}} \quad (20)$$

Each bearing has two points of contact. To find an overall damping coefficient for the system, the damping coefficient for each point of contact must first be found. Firstly, consider the bottom point contact where the bearing meets the core floor as in Figure 1 on page iii. Adding together the vertical force components led to the following:

$$N_1 = m g + F_d \sin(\alpha) \quad (21)$$

Where  $N_1$  is the normal force at the first node considered,  $F_d$  is the force due to a mounted mass on a single bearing within the footer, and  $m g$  is the weight of the tungsten carbide 10 mm bearing.

The normal forces at the second point of contact equal the force due to the mounted mass. However, this interaction needs to be translated into the same plane as the velocity. This yield the following expression for its normal force:

$$N_2 = F_d \sin(56.31^\circ) \quad (22)$$

The damping coefficient due to the bottom contact and top contact could then be calculated using equation b.19. Summing these coefficients gives the coefficient of friction for each bearing  $c_{bearing}$ :

$$c(\text{bearing}) = \frac{\mu N_1}{v} + \frac{\mu N_2 \sin(56.31^\circ)}{v} \quad (23)$$

$$= \frac{\mu}{v} (m g + 2 F_d \sin(56.31^\circ)) \quad (24)$$

The next step was to scale this value to the whole system and then the damping factor for any particular preload and mass can be calculated using Equation 17. The value was thus multiplied by the total number of bearings in three footers.

By applying Equation 17 and 18 the system's damping factor and damped natural frequency can be found. Still using the systems arbitrary dimensions and assuming an average driven velocity of  $0.837 \text{ m s}^{-1}$  (measured in initial experimentation), a graph of the preload against the maximum and minimum damped natural frequency could be plotted as shown in Figure 20.

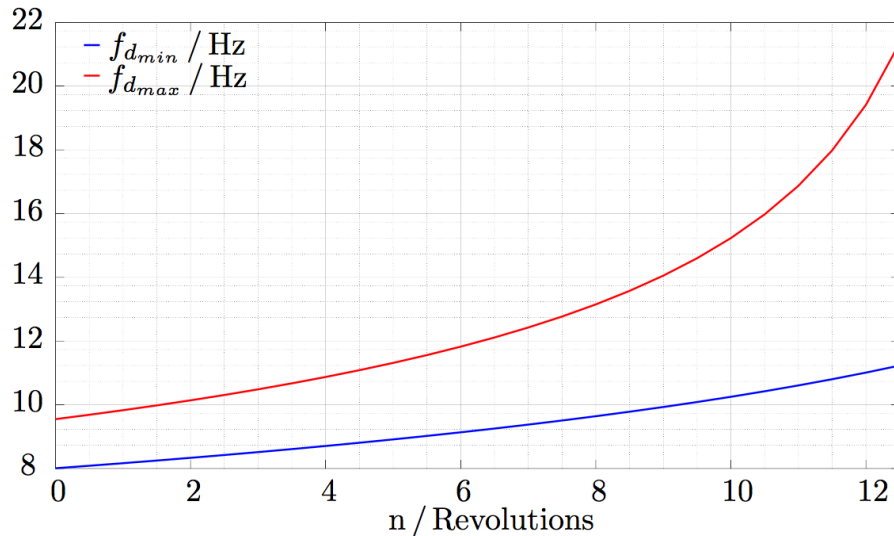


Figure 20: Graph of pre-load against its corresponding maximum and minimum damped natural frequency (Hz).

Now in Figure 20 the lines representing the maximum and minimum damped natural frequency act as an envelope. The mount could operate at any value within this envelope. The boundary conditions of 8 Hz–12 Hz can be added to the graph (see Figure 21) and are represented as black dashed lines.

The limits of 8 Hz–12 Hz can be translated into our Pre-load vs Mass resting on three feet graph (figure 22). The Frequency boundaries are again represented by the black dashed lines.

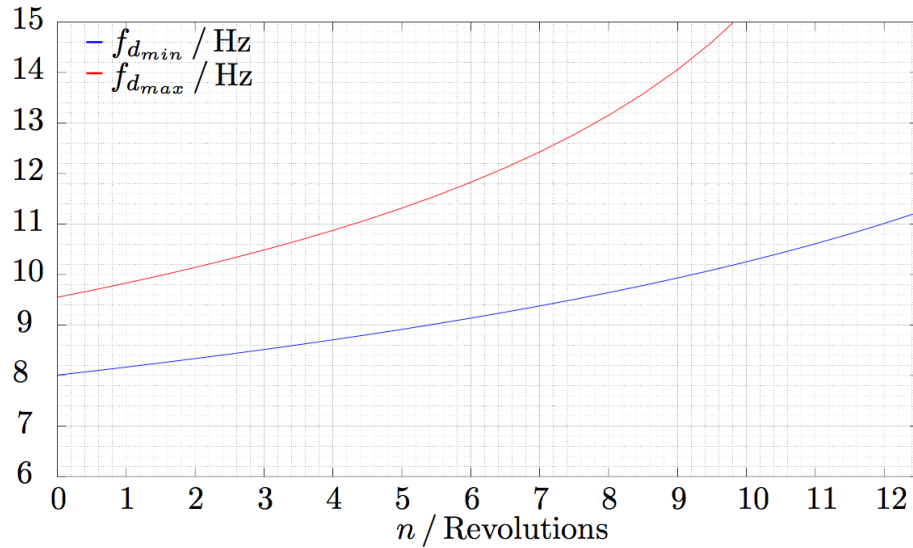


Figure 21: Graph of pre-load against its corresponding maximum and minimum damped natural frequency (Hz), and the 8 Hz–12 Hz boundary represented.

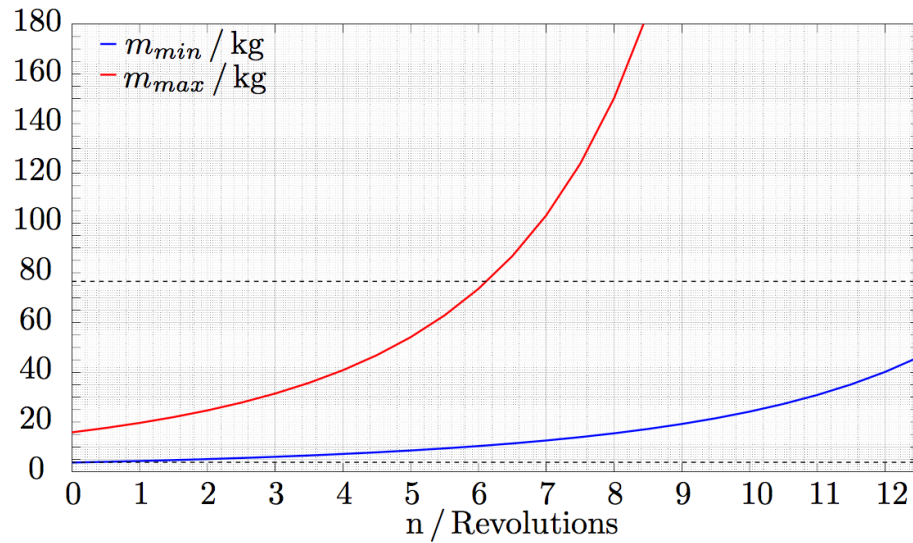


Figure 22: Graph of pre-load vs the maximum and minimum supported mass on three footers, with the 8 Hz–12 Hz boundary frequencies represented as boundary mass values.

Finally, these conditions were considered for preload against damping factor. A similar set of envelopes was produced:

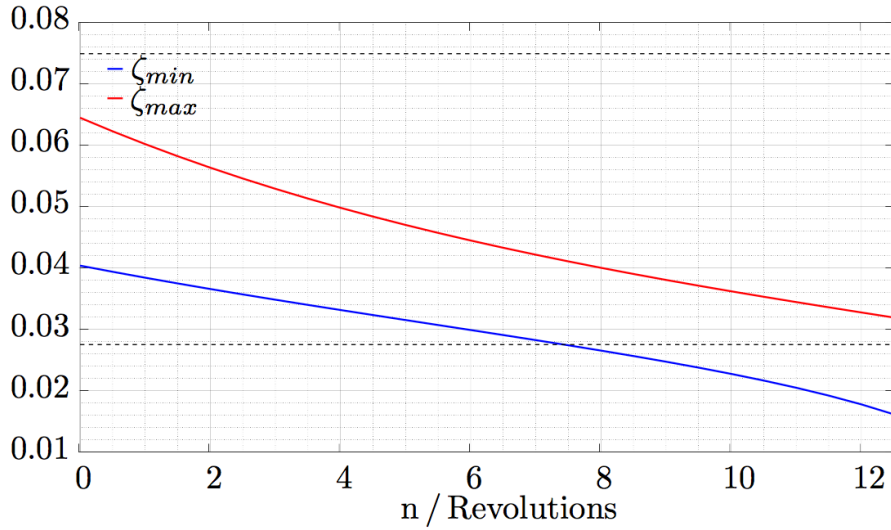


Figure 23: Graph of pre-load vs the maximum and minimum damping factors for a system of three footers. The 8 Hz–12 Hz boundary frequencies are represented as boundary damping factor dashed lines.

For both Figures 21, 22 and 23, the area contained within the two envelopes represents the operating area of the system.

### 3.6.2 System Tuning

With a mathematical model implemented, the values of the parameters can easily be changed, making fine tuning the internal mechanism very straight forward. After testing a range of values for each governing parameter, the ideal mount dimensions and magnet properties were found. With the intention of maximising the operational area contained within the previous enveloped graphs, a final set of preload graphs were plotted—see Figures 24, 25 and 26.

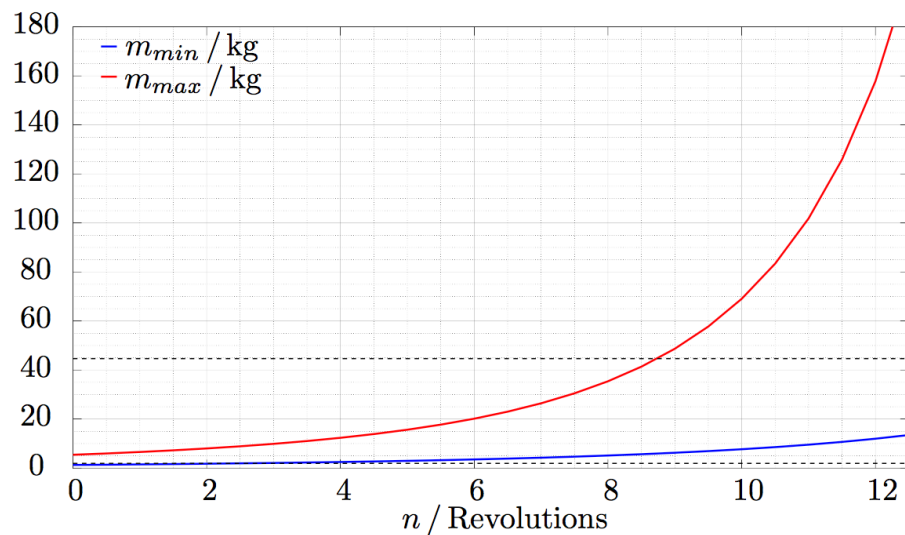


Figure 24: Preload against optimised mass operational area.

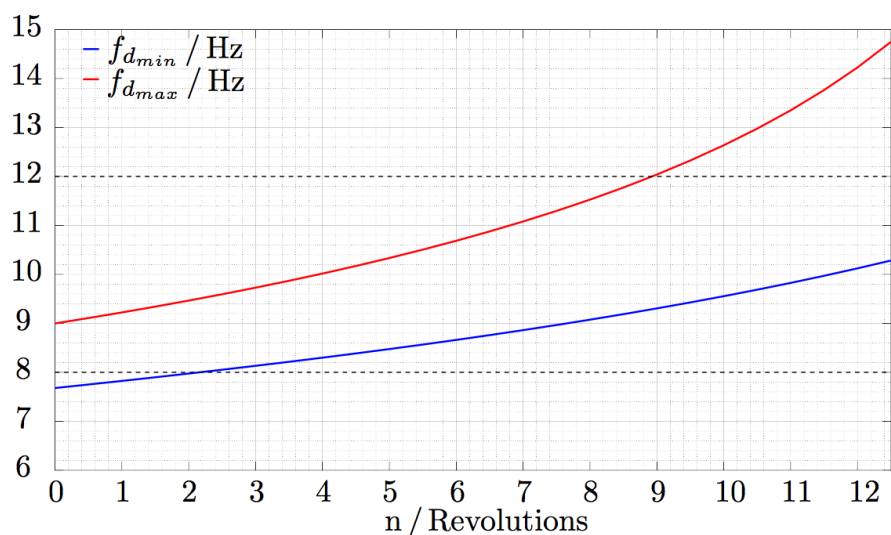


Figure 25: Preload against optimised damped natural frequency operational area.

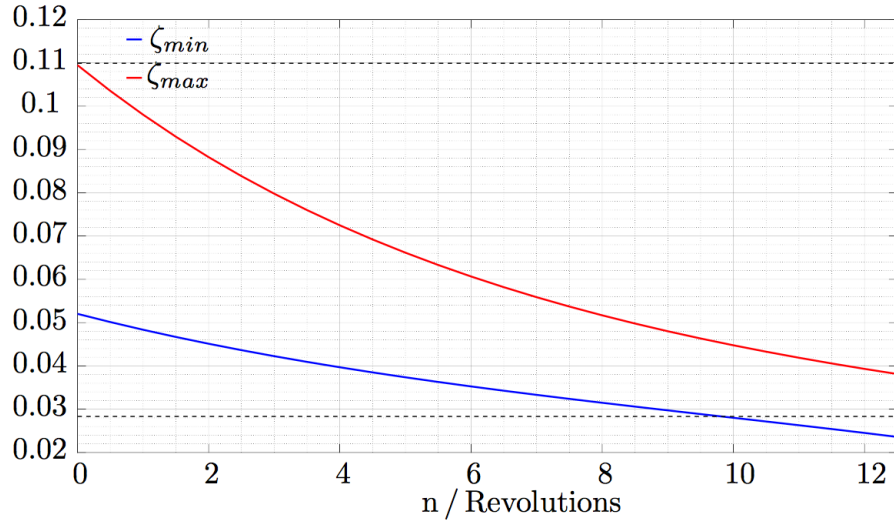


Figure 26: Preload against optimised damping factor operational area.

The user should be able to select a desired preload for any specific values of mass within the operational area. To do this a technical graph of mass-preload was produced as in Figure 27, and will be provided to allow a system preload to be easily selected.

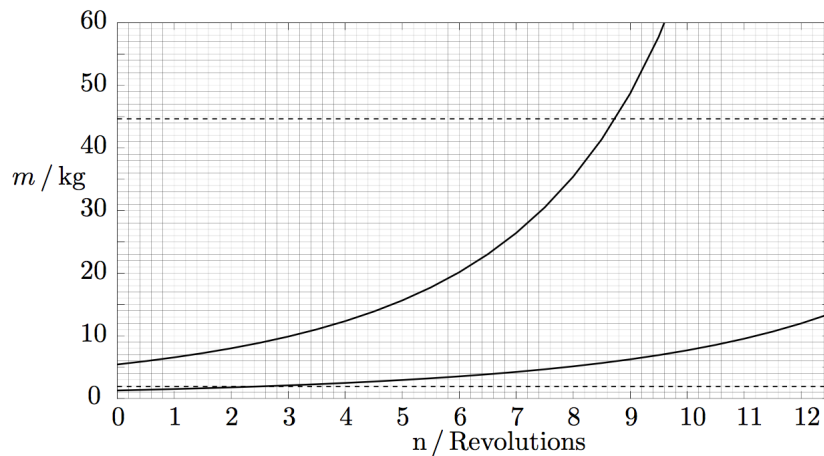


Figure 27: Preload vs rated mass of a mounted device on three footers.

Now, for the any particular selected mass the system will have a specific damped natural frequency and damping factor. The user can read off these system details using a further two technical graphs, Figure 28 and Figure 29.

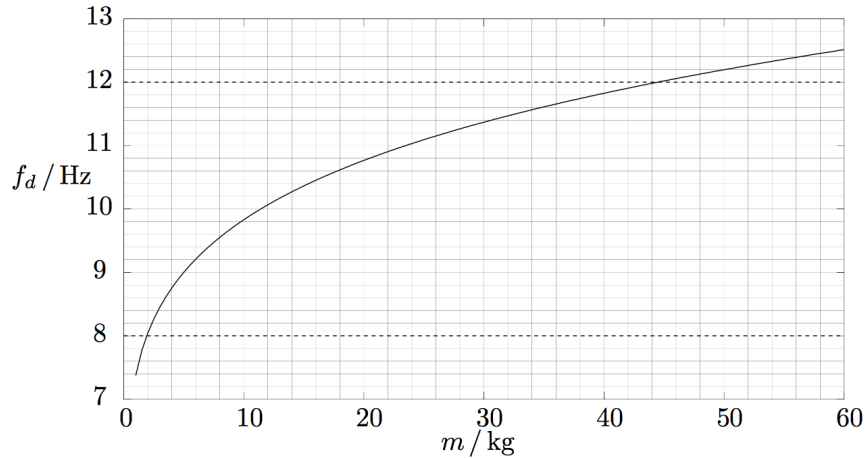


Figure 28: Rated mass on three footers vs corresponding system damped natural frequency.

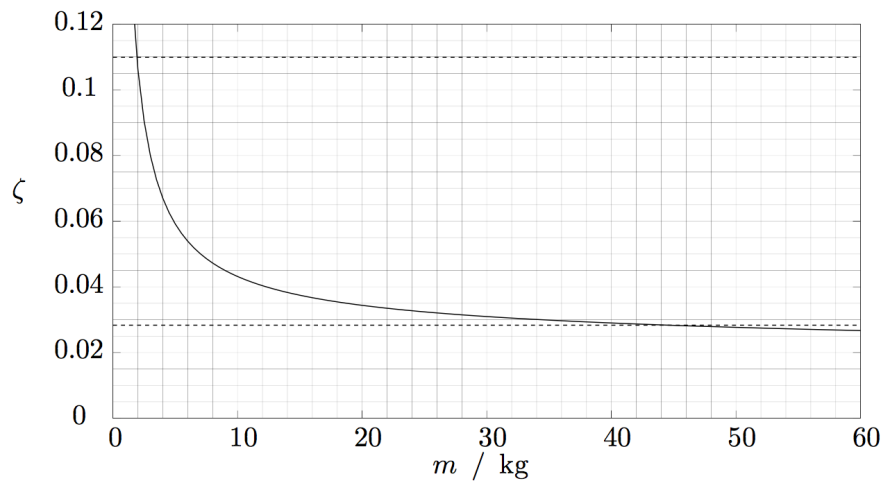


Figure 29: Rated mass on three footers vs corresponding system damping factor.

### 3.6.3 Experimentation

To assess the effectiveness of the product, acceleration data from a vibrating amplifier was recorded to determine the frequency content of the signal to be attenuated. The same setup was used to capture acceleration data from the amplifier when mounted on half squash balls, which was later compared to the output of a dynamic model representing the final mount design using the undamped acceleration data captured as the model input. Squash balls were used to isolate Hi-Fi systems before footers entered the market and are an entry level alternative to footers.

A USB PicoScope<sup>2</sup> was used to capture the output of an accelerometer<sup>3</sup> at a sample rate of 50 kHz for 10 s. Human hearing ranges from 20 Hz–20 kHz; according to Nyquist, the sample rates had to be at least twice 20 kHz to determine the power of these frequency components.

The accelerometer was coupled to the top of an amplifier connected to a standard AC mains power supply—nominal voltage of 240 V at a frequency of 50 Hz. Data from the accelerometer was captured for three conditions: with the amplifier turned off, on, and the amplifier turned on whilst sitting on half squash balls.

The data captured came in the form of a voltage output. To determine the acceleration from this information it was necessary to form a transfer equation. To do so, the technical data sheet for the accelerometer [15] was found and in it there was clear conversion which lead to the following

$$\ddot{y} = 9.81 \cdot (0.66 \cdot V - 1.65) \quad (25)$$

where  $a$  is the acceleration in  $\text{m s}^{-2}$  and  $V$  is the voltage measured in V. Equation 25 is linear, so has no affect on the shape of the spectra. The spectra of the measured voltages were analysed instead.

Firstly, the data for the amplifier when off—the control—was compared to the amplifier when on; There were no observable components above the noise floor in the range 1 kHz–25 kHz.

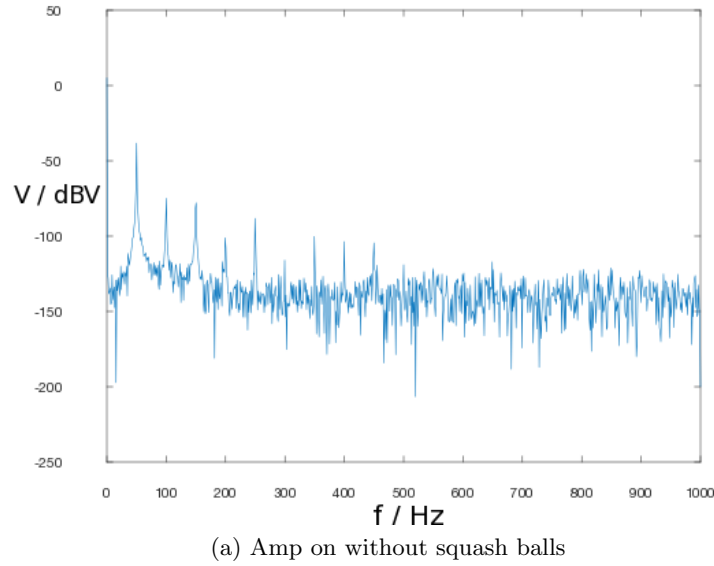
The spectra for amplifier when off had a fundamental at 50 Hz. This is likely due to interference from other mains powered devices in the room—air conditioning, PCs and desktop power supplies for example. Contrasting this control spectra to the spectra for the amplifier when turned on, the fundamental frequency increased in power significantly from  $-90 \text{ dBV}$  to  $-40 \text{ dBV}$ —a factor of  $10^5$ . The harmonics can be seen at 50 Hz intervals although the noise floor due to the error of the accelerometer remained at  $-140 \text{ dBV}$ .

Next, the spectra for the amplifier when on was compared to the spectra for the amplifier damped using squash balls. Figure 30 on the following page reveals the effect the squash balls had on the frequency content of observed vibrations.

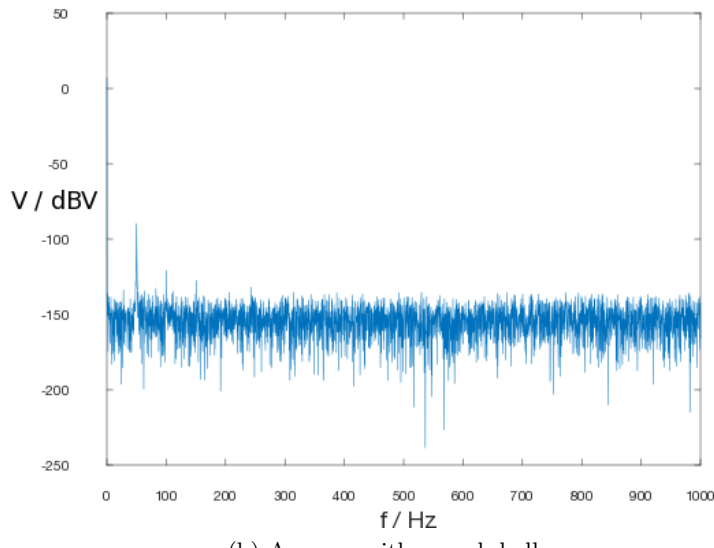
---

<sup>2</sup>Pico Technology PicoScope 2204A

<sup>3</sup>STMicroelectronics LIS344ALH



(a) Amp on without squash balls



(b) Amp on with squash balls

Figure 30: Compared Frequency Responses with and without Squash Balls

The fundamental remains constant in frequency and power. However, from the simple damping the squash balls provide, the noise has been significantly cleared up, along with this success the harmonics have consistently lower peaks. This provides an example of successful damping which can be used as a comparison to the later mathematically damped data using dynamic model. The aim is to further clean up the noise and lower the power of the harmonics as much as possible, preferably below the noise floor

which should lead to a reduction in microphonic effects and increase in sound quality.

### 3.6.4 Dynamic Simulation

It was determined that a dynamic model of the system would be necessary to quantify the potential success of the product. This could visually display the effects of the footers on attenuation of a signal from a Hi-Fi system, and hence inform whether the sound quality would be improved.

The three footers and mounted equipment can be simplified to a spring-mass damper system with non-linear stiffness—a driving force  $F_d$  is supplied by the vibration of the Hi-Fi system, and the opposing forces from the magnetic repulsion force  $F_m(y)$ , damping force  $c\dot{y}$  and system inertia  $m\ddot{y}$ . Considering these components, it was possible to develop a second order differential equation which when solved would characterise the effectiveness of the footers.

$$F_d = m\ddot{y} + c\dot{y} + F_m(y) \quad (26)$$

Simulink® was chosen to drive the dynamic model due to the straightforward construction of differential equations it provides; it offers a visual representation of the system and works hand-in-hand with MATLAB™ allowing for simple data processing. Simulink computes an iterative numerical solution and outputs a corresponding time series to the MATLAB workspace which can be transformed into the frequency domain for analysis.

Four components needed to be defined to complete the model:

- The mass of the supported equipment and top piece  $m$ . The simulation was run on the nominal supported mass of 20 kg.
- Constant  $c$ , which is dependent on the supported mass and the frictional coefficient  $\mu$  between the tungsten carbide balls, and stainless steel cones and races for all three footers.
- A transfer function  $F_m(y)$  to find the magnetic repulsion force given the vertical displacement of the equipment.
- $F_d$  which varies with time and the input to the system, found by applying Newton's second law to the undamped accelerations measured in Section 3.6.3.

Section 3.6.1 details how the magnetic repulsion force can be calculated given the vertical displacement of the equipment using Equation 7 after translating the vertical displacement into the displacement of the bearings. This was implemented as a subsystem in Simulink, incorporating transformations necessary to determine magnet separation given horizontal displacement; repulsion force acting on a single bearing given magnet separation; and total reaction force given the force acting on a single bearing.

Ideally the damping coefficient for various masses would be determined empirically, however, using the theoretical approach outlined in Section 3.6.1 the damping coefficient was found for a range friction coefficients  $\mu$ . Typically for these materials  $0.4 < \mu < 0.6$  [10]. Substituting the limits and nominal mass into Equation 23 on page 21, the damping coefficient was bounded as follows:

$$159 \text{ N s m}^{-1} < c < 238 \text{ N s m}^{-1}$$

Figure 31 displays the top level model architecture. The topology is typical of spring mass damper systems as detailed in [16].

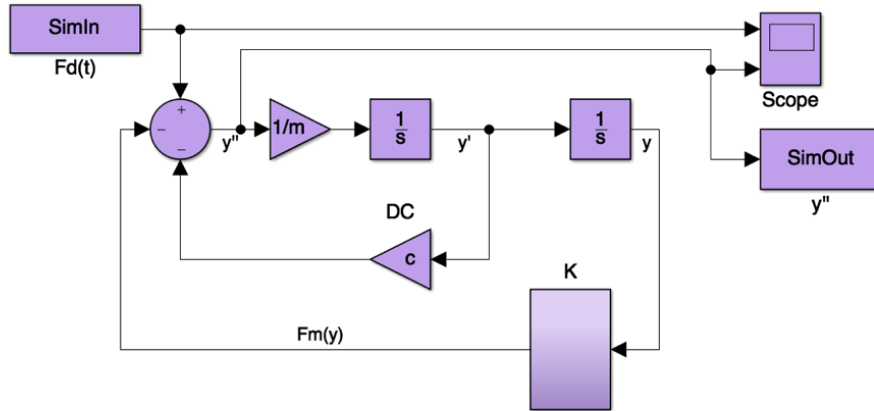


Figure 31: Dynamic model used to verify the performance of the footer.

The constant stiffness was replaced with the subsystem used to find the magnetic repulsive force. *SimIn* provided an interface to the MATLAB workspace which was used to input the driving force. Similarly, *SimOut* exported the system output to the workspace; the acceleration of the equipment as a time series. Using the inverse of Equation 25 on page 28, the model output was converted into voltages so its spectra could be compared to the accelerometer output measured for the undamped amplifier.

Figure 32 on the following page shows the effect of running the simulation with the damping coefficient at each extreme.

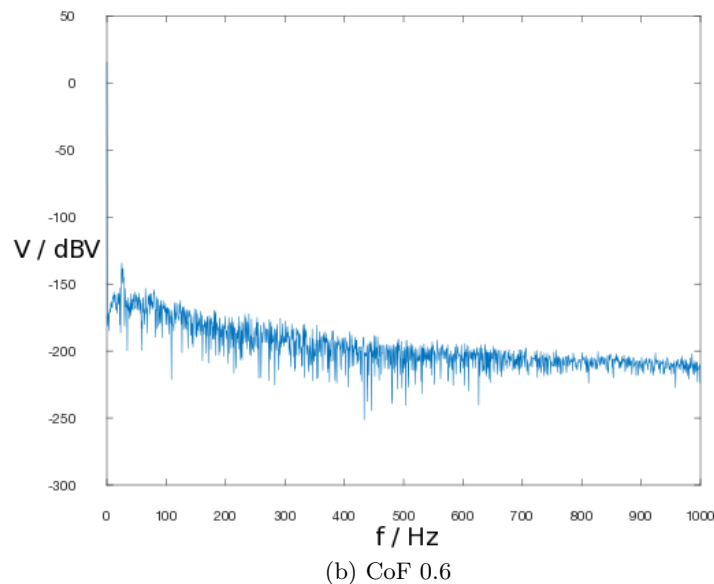
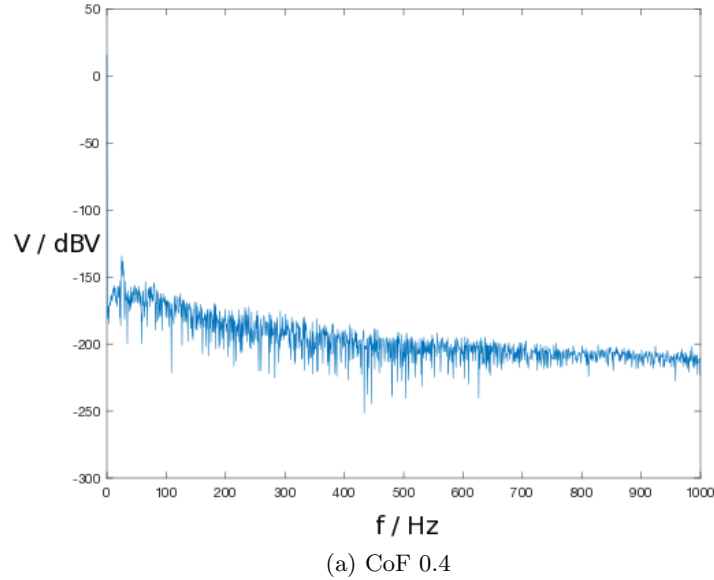


Figure 32: C6—Alternative cone and bearing concept.

In both graphs, the fundamental frequency can no longer be observed; a peak at around 30 Hz is apparent however its low power and frequency that differs from 50 Hz indicate that this is just noise. The noise is effectively identical in both cases and hence it can be concluded that the difference in damping coefficient across its range negligible effect. For further analysis, the median coefficient of friction will be used—0.5—this returns a damping coefficient of  $198 \text{ N s m}^{-1}$ .

The undamped is displayed with the simulation output damped spectrum for comparison between the input and output of the dynamic model in Figure 33.

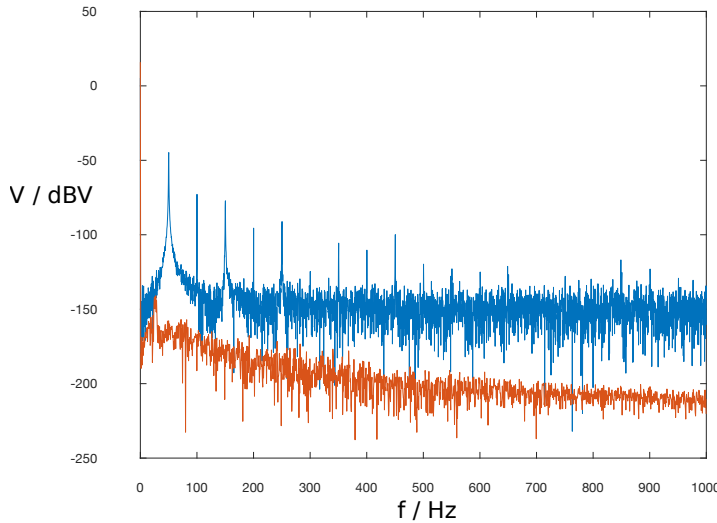


Figure 33: Comparison of Undamped and Damped Response

The red curve shows the simulation output; the fundamental frequency and its harmonics are indistinguishable from the noise. The entire signal has been reduced to below the noise floor of around  $-140$  dBV. The noise has been almost completely attenuated.

The success of the footers is likely to be less significant than that of the model. The primary reason for this discrepancy is the value of damping coefficient used. Ideally, this would be found empirically; a series of prototypes would be produced and a similar experiment carried out to find the true damping coefficient.

If the footers have a fraction of the successs they have been predicted to have, there will be a significant improvement in sound quality.

## 4 Design for Manufacture

DFM defines the design of a product so as to best optimise its quality whilst minimising its cost to manufacture. Factors affecting this cost include the number of off-the-shelf and machinable parts, the set-up time of required machinery, the material type, dimensional tolerances as well as secondary processes. Generally, a compromise is reached between the functional quality of a product and the cost of manufacture however, considering the current extortionate pricing of similar existing products, certain design choices have taken precedence over their implications in a manufacturing context. For

example the rails within the complex central piece—part number COR080-0003—are expensive and difficult to manufacture yet optimal for the specified mechanism.

#### 4.1 Bill of Materials

Figure 34 labels all of the parts used in the final design, including the user replaceable parts sold separately: the spike and base. These are described in Table 3.

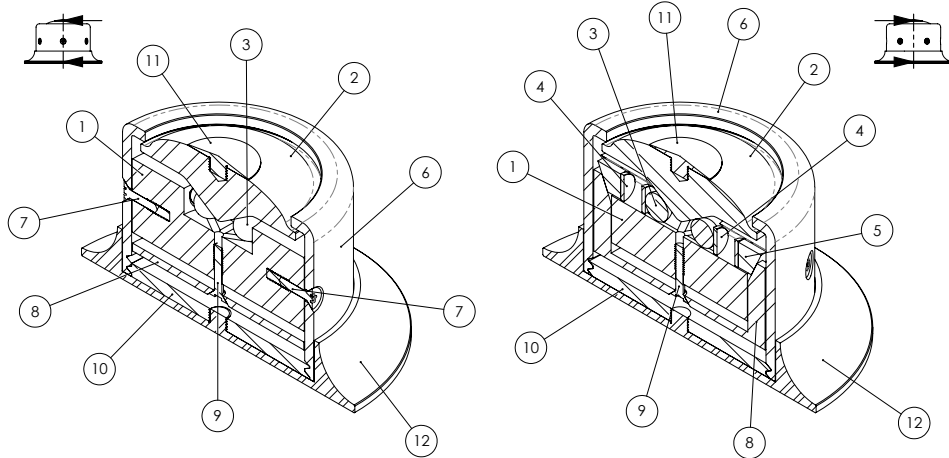


Figure 34: Item numbers for Table 3.

Table 3: Bill of Materials

| Item No. | Part No.                       | Description   | Qty. |
|----------|--------------------------------|---|------|
| 1        | COR080-0003                    | Isofonics core piece                                | 1    |
| 2        | TOP080-0004                    | Isofonics top piece                                 | 1    |
| 3        | 10MMTUNGSTENBALLS <sup>1</sup> | ø10 mm tungsten carbide ball                        | 6    |
| 4        | F669-N45SH-10 <sup>2</sup>     | ø10 x 1.5 mm neodymium button magnet                | 12   |
| 5        | PLD010-1004                    | Isofonics preloading back-stop                      | 1    |
| 6        | RET080-0003                    | Isofonics retainer                                  | 1    |
| 7        | M4X20-CSK-ST <sup>3</sup>      | M4 x 20 mm T20 A2 c'sunk screw with partial thread  | 6    |
| 8        | PLD080-0003                    | Isofonics preloading crown                          | 1    |
| 9        | M4X20-CSK-H <sup>4</sup>       | M4 x 20 mm H2.5 A2 c'sunk screw with partial thread | 1    |
| 10       | RET080-1002                    | Isofonics retainer bottom                           | 1    |
| 11       | USR080-0001                    | Isofonics removable spike                           | 1    |
| 12       | USR080-1002                    | Isofonics removable base                            | 1    |

<sup>1</sup> <http://www.vxb.com/10mm-Tungsten-Carbide-Bearing-Ball-0-3937-inch-Dia-p/10mmtungstenballs.htm>

<sup>2</sup> <http://www.first4magnets.com/circular-disc-rod-magnets-c34/>

10mm-dia-x-1-5mm-thick-n45sh-neodymium-magnet-1-lkg-pull-p3633

<sup>3</sup> [http://www.westfieldfasteners.co.uk/A2\\_ScrewBolt\\_PinTXCsk\\_M4.html](http://www.westfieldfasteners.co.uk/A2_ScrewBolt_PinTXCsk_M4.html)

<sup>4</sup> [http://www.westfieldfasteners.co.uk/A2\\_ScrewBolt\\_SHCsk\\_M4.html](http://www.westfieldfasteners.co.uk/A2_ScrewBolt_SHCsk_M4.html)

Due to the complex geometry required from our design, only a few components may be bought in: items 7 and 9, screws sourced from Westfield Fasteners, a UK retailer which deals in volume production; item 4, the neodymium magnets sourced from first4magnets who distribute worldwide; item 3, tungsten carbide ball bearings sourced from a wholesale UK retailer VXB bearings. The tungsten carbide ball bearings are a specialist part. Table 3 details exact source and the quantity required per mount.

All parts are to be machined using a 3 axis CNC mill excluding the item 1, which also requires wire erosion. Wire erosion is considerably more expensive but allows for the more intricate designs required by this piece. Forging was considered as a method of manufacture but was dismissed for the following reasons; the large expenditure involved in machinery, dies, tools and personnel are only justifiable for large scale production and the die accuracy required to forge the most complex pieces is likely unachievable. In the interest of reducing manufacturing cost, for which the complex geometry of the core piece is largely responsible, it was proposed during discussion with Sylatech Ltd.® that the piece be machined in separate parts that are later joined to avoid the machining of reverse chamfers as shown in Figure 35.

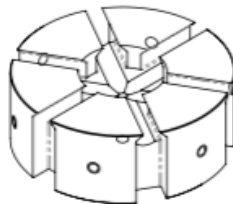


Figure 35: Core

Cost is substantially driven by time; time to remove material in the machining process as well as set-up time of the machine itself. Conveniently, our design is highly symmetrical meaning time and money is saved through lacking the need of a complex orienting mechanism given that the part's orientation prior to machining is irrelevant.

Finally, the volume of production is of great importance; with too small a batch size, set up costs and jig production costs become impractical and with too large a batch, storage costs pose a problem for a product of which the market response is not easily predictable. Considering the high cost and exclusive appeal of this product, low volume batch production in the order of 100 is appropriate so as to eliminate any unnecessary storage costs and allow adequate response to market needs. Specifically a volume of 300 pieces has been defined because it is divisible by three, the mounts are expected to be sold in groups of three, and during correspondence with Sylatech Ltd., it was discussed that any larger batch volume would pose an infeasible machining time; namely roughly two weeks.

## 4.2 Finishes

A range of finishes best suited to individual parts have been chosen based on its functionality and location. A relatively cheap 2B (basic smooth) finish is to be applied to the stainless steel core so as to prohibit unnecessary expenditure considering the part shall not be seen by the customer whilst ensuring a path of minimal friction exists for the moving ball bearings. Additionally, the standard aluminium mill finish is rough and so all internal aluminium preloading pieces are to be brushed in the direction the piece travels so as to limit the amount of wear. Furthermore, the external retainer is to be brushed in concentric circles to give an attractive finish and hide any scratches. A 2J finish is to be applied to all other external stainless steel pieces as it is cheaper to produce than polishing and is practical in that it is resistant to scratches whilst being aesthetically pleasing [17].

All parts are to be machined at fine linear and angular tolerances of  $\pm 0.1$  mm and  $\pm 1^\circ$  respectively to ensure the overall quality of the product. However there exists opportunity for optimisation within this section; in the interest of reducing cost, it was concluded that the rails contained in the core piece are the only parts to be machined to a high tolerance since they are to fit plush to the bearings; all other parts may be machined to a coarser, and therefore cheaper, tolerance.

## 4.3 Manufacture Costs

### 4.3.1 Optimisation

Sylatech Ltd<sup>®</sup>, a machining company situated in the North East of England, was contacted regarding the cost to manufacture the product and proved very informative with regard to the feasibility of our product. Initially a cost of roughly £500 per piece (for a batch volume of 300) was quoted which, allowing for appropriate margins detailed in Section 7.3, dictates a retail price of £1 650. The most expensive existing product of similar concept is priced at £849.99 and, although our original product features merit a higher retail price, a difference of roughly £800 is too large when introducing a new product to the market.

The following suggestions were made to reduce the quoted figure;

- The rails of the core piece were to be modified such that the radius of the bearing race was continued until tangential with the wall. Simply, the right-angles depicted in Figure 36 were to be removed. This revision was quoted to save roughly £100 per mount.
- The 0.3mm dimension of the base as shown in Figure 37 was to be extended to 2 mm; the larger dimension is easier to grip and therefore would require less delicate and costly machine handling. This change was quoted to save roughly £10 per base.

- The retainer was to be machined using a 4 axis CNC machine which is considerably faster because fewer operations are required. This change was quoted to save roughly £20 per piece.

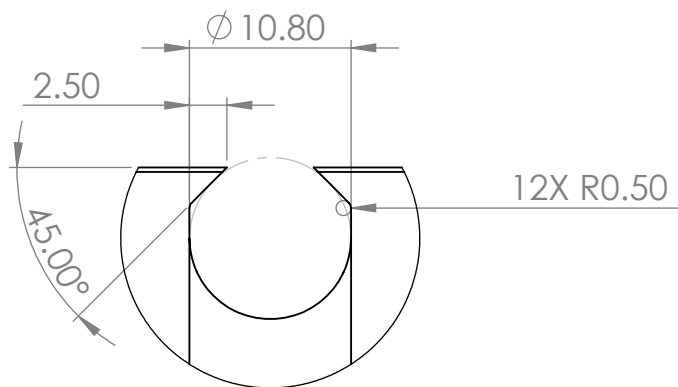


Figure 36: Bearing race cross-section drawing

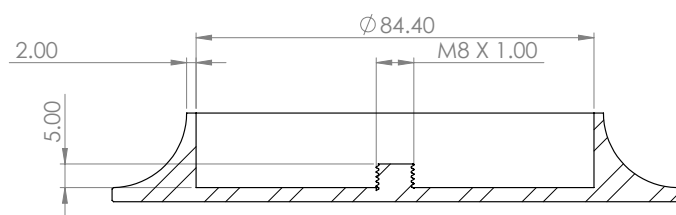


Figure 37: Base cross-sectional drawing

### 4.3.2 Costing

Table 4: Costing

| Item No. | Part No.                              | Qty. | £/Piece | £ Total             |
|----------|---------------------------------------|------|---------|---------------------|
| 1        | COR080-0003                           | 1    | 97.00   | 97.00               |
| 2        | PLD080-0003                           | 1    | 35.00   | 35.00               |
| 3        | PLD010-1004                           | 6    | 2.00    | 12.00               |
| 4        | F669-N45SH-10<br>(first 4 magnets)    | 12   | 0.30    | 3.60                |
| 5        | 10MMTUNGSTENBALLS<br>(VXB Bearings)   |      | 20.30   | 121.80              |
| 6        | TOP080-0004A                          | 1    | 32.50   | 32.50               |
| 7        | RET080-0003                           | 1    | 25.00   | 25.00               |
| 8        | M4X20-CSK-ST<br>(westfield fasteners) | 6    | 0.09    | 0.54                |
| 9        | M4X20-CSK-H<br>(westfield fasteners)  | 1    | 0.04    | 0.04                |
| 10       | USR080-0002                           | 1    | 14.30   | 14.30               |
| 11       | RET080-1002                           | 1    | 12.00   | 12.00               |
| 12       | USR080-1002                           | 1    | 20.00   | 20.00               |
|          |                                       |      |         | 373.78 <sup>1</sup> |

<sup>1</sup> Quote courtesy of Sylatech Ltd.

Table 4 details the final cost of off-the-shelf parts and machining per mount, totalling £373.78 per mount.

## 5 Design for Assembly

### 5.1 Jig Design

Due to the small scale of our product, hand assembly is required. Considering the complexity of the design and physical impracticality of overcoming the repulsive magnetic forces during its assembly, a jig has been designed, as shown in drawings JIG080-0001 and JIG080-1001, with full accompanying assembly instructions—see Appendix C.

### 5.2 Assembly Costs (E.O. HOLLANDS)

Considering the assembly jig is to be re-used, its cost is negligible within the context of the product's assembly. Assembly costs are then only defined by the time taken to manually assemble the device and the cost of manual labour which can be estimated at 2 minutes and £8/hr respectively. This equates to a total of £0.27 per piece.

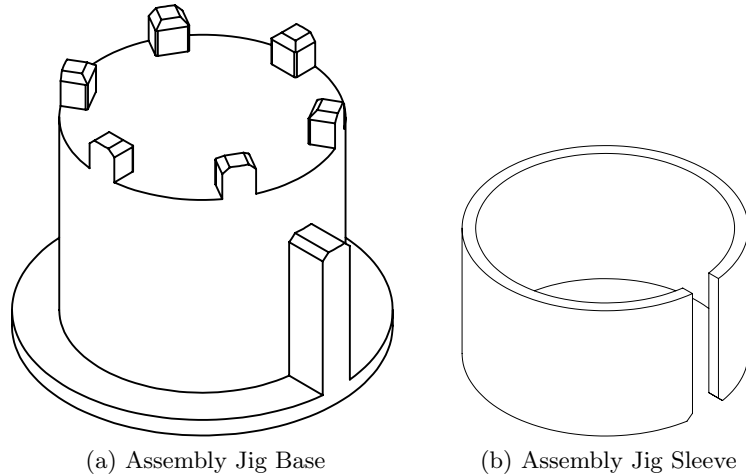


Figure 38: Assembly Jig Components

## 6 Design for Sustainability

Isofonics recognises the importance of considering the environmental implications of the manufacture as well as disposal of any product.

Isofonics footers are made to last a lifetime. This is achieved by using the highest quality materials possible; quality and endurance were more important than the price of the product considering the high budget of the design. This reduces the harm done to the environment by eliminating the need to manufacture replacement footers. Another method of ensuring minimal impact is to reduce the scrap, this is achieved by ensuring that the size of the raw material is a similar size to the final product. The main central section of the footer is produced using a CNC machining process as described previously and so the un-refined steel will be cut to within a small tolerance of the final product. The scrap that is inevitably produced will be recycled; this includes both stainless steel and aluminium.

Stainless steel contains valuable raw materials, especially chromium, nickel and molybdenum and hence recycling it is economically viable. Like many other metallic materials, stainless steel is recycled through a re-melting process, where the melted steel is re moulded for use. Similarly, aluminium is also recycled with a re-melting process and can be reprocessed and reformed endlessly without losing any of its quality.

Packaging often contributes to the waste generated by the product; to avoid this, the footers will be packaged in simplistic cardboard based materials which can be efficiently recycled rather than plastics where the recycling process yields less useful products.

## 7 Commercial Considerations

### 7.1 Brand Development and Competitor Analysis

With the intention of establishing the design in the market, a brand identity was essential. Through several brainstorming sessions, the team agreed on the name *Isofonics*.

It was important to review the current market leaders, Stillpoints and Nordost, with their relevant products. Nordost primarily manufactures Hi-Fi audio cables but recently introduced additional products for resonance and power control. Namely, their Sort Kone acts as a vibration drain with a mechanical diode effect to prevent external vibrations from travelling up through the cone. Similarly, three cones are recommended per device but they offer 3 types of cone, each made from different materials. The most expensive is made from titanium and utilises ceramic bearings, retailing at £349.99 per cone. Stillpoints offer an equivalent solution, their most expensive is their Ultra 6, priced at £799.99 per mount and £849.99 with an accompanying base [18].

### 7.2 Stillpoints Patent Check

Stillpoints' patent for their *Universal Vibration Damper* was thoroughly studied and the potential risks of infringement were identified.

#### Parallels with Stillpoints

The following details the main claim made by Stillpoints and highlights areas of concern:

'A device for the control of vibrations comprising: *a retainer*, the retainer constructed and arranged to rest upon a base, at least a portion of the base defining *a substantially flat surface*; and *a plurality of bearings* disposed within the retainer, the bearings arranged in *a first layer and a second layer*, the second layer disposed on the first layer, the first layer comprising three or more bearings, and the second layer comprising at least one bearing, each bearing in the first layer constrained on its bottom by only the substantially flat surface of the base, on its side by the retainer, the bearings in the first layer supporting the at least one bearing in the second layer, the retainer defining a surface which is in substantially tangential contact with the bearings in the first layer' [19]

It is clear that the main claim focuses on the use of layers of bearings, in this way, our design is fundamentally different. Since our design differs from that outlined in the main claim, all further claims based on the first are irrelevant. An element of originality of our design lies in the use of magnets which is not mentioned at all within the official claims section of the patent.

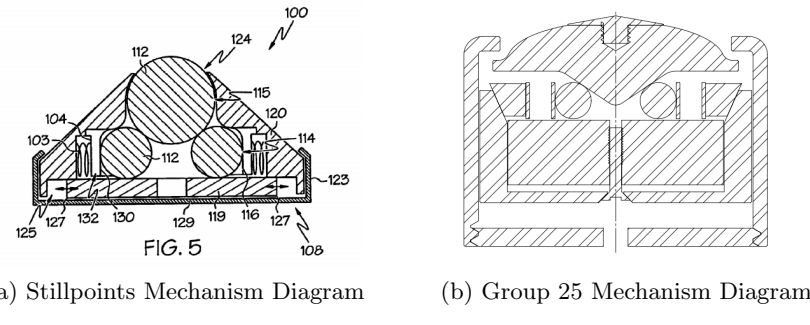


Figure 39: Stillpoints Mechanism Comparison

To verify that the mounts did not bear a resemblance to Stillpoints' invention, Robin Bartle, a patent lawyer from Bartle Read, a company based in Liverpool which specialise in intellectual property was contacted who was able to confirm that 'Because the mount does not feature a second layer of bearings as shown on the cross-section, there are no blatant overlaps between the two products and Stillpoints would not have sufficient grounds to sue'—see Figure 39. Additionally, Mr Bartle noted that this is a US patent and is not filed with the European Patent Office and so would only stand to limit sales within the US.

### Points of Originality

- Use of *opposing magnetic fields* for lateral damping as opposed to springs
- *Cone* with retaining flange replacing layers of bearings
- *Pre-loading mechanism* in which a screw in tension moves a fixed magnet decreasing its distance from the bearing magnet thus increasing the strength of the system—adjustable for a variety of masses.

### 7.3 Marginal Costs

With reference to Table 4, and accounting for assembly costs as discussed in section 5.2, the main contained mechanism, optional base and spike are to cost roughly £340.00, £20.00 and £14.30 respectively to produce.

With respect to production costs, margins of 100% for product distribution, 100% for retail and 30% for profit are to be met which consequently dictate the following retail prices. The main device shall retail for £1 149.00, the optional base for £66.00 and the removable spike for £49.00.

## 8 Discussion

### 8.1 Specification Fulfilment

In order to evaluate how the design outcomes of this project met the reflected the specification points, the three main headings of the URS tree in Figure 2 on page 1 were assessed individually as follows.

#### Eliminate Microphonic Effects

The requirement for a rigid load path was integral to the performance of the damping mechanism. The interaction between the magnets and the spherical bearings in conjunction with the hardness of their material diminished the excess mechanical vibrations generated by microphonic effects as demonstrated by the graphs produced by the dynamic model. However, the data yielded during the experiment which was then inputted to the simulation, did not fully reflect the execution of the design and is therefore a source of uncertainty. Employing

the squash balls as a method of dampening the noise produced by the amplifier did validate the concept but would be of more value if a prototype was used to establish a value empirically.

#### Budget Constraints

With reference to the commercial considerations section and design for manufacture, it is clear that the market for isolation devices is not driven by cost, instead by sound engineering science. However, in comparison with the products introduced by Nordost and Stillpoints, the cost for one mount differs substantially and so must be justified. For example, there is a £300 difference with Stillpoints Ultra 6 mount with the original costings. The advantages over these competitors are as follows:

- Provide proof of concept through dynamic model.
- Appeal to hobbyists through hands-on 'tweaking' graphs.
- One set of mounts accommodates a range of masses. More do not need to be bought for heavier/lighter devices, unlike with Stillpoints.
- Use of premium materials, namely tungsten carbide bearings.
- M8 threads at the top and bottom pieces allow the user to amenably couple their device to the footers.

### Integrate with existing equipment

The HiFi equipment must only rest on three footers to prevent further resonances and heating in the arrangement. If another was used, it would either prove redundant or induce further noise. The cone provided a single point of contact which in turn meant that 3 footers were needed to support one piece of equipment. Partnered with the large base plate, this guaranteed that the mounts would not slip and the system was amply stable. In addition, the aesthetically pleasing finishings ensure that the footer is well integrated with the existing system and is resistant to scratches. On the other hand, it could not be proven that the mount avoids blemishing because a prototype was not made and tested over a sufficient amount of time.

## 8.2 Further Developments

In the interest of expanding the design beyond the scope of this project, a number of proposals have been made:

- A product family can be produced. This would consist of a variate of differently rated footers which would be optimised for different mass ranges. This could be achieved easily by varying the mount dimensions and magnet properties. This would allow for the mounts to support a wider range of heavier equipment such as loudspeakers.
- A companion phone application which enables the user to adjust the preload for a desired mass. This could be a simpler aid than the provided preloading graphs produced from the parametric model.
- Modelling the magnetic flux within the system using a 3D finite element analysis software. This would allow for a more accurate consideration of the magnet interactions and flux distribution within the mount. Specifically it could improve the parametric model which is based on the assumption that there are no interactions between adjacent pole pairs.

## 9 Conclusion

The following statements summarise the main results of the project:

- The URS tree provided a sound and comprehensive depiction of the brief.
- Suitable engineering techniques were applied. 2D finite element analysis software was employed to model magnetic flux distribution and confirmed there was no harmful leakage from the system. The internal mechanism was also statically and dynamically analysed to determine

the effect of preloading the system and consequently, the noise attenuation.

- Numerous progressive iterations of the model were produced. These acted as successively improved revisions of the design to include, for example, the top piece and threaded spike.
- The manufacturing considerations were researched and processes were modified following professional feedback that some parts were too expensive or too complex to machine.
- A prototype must be made and tested to provide additional proof of concept. This will yield a more accurate rating for noise attention and hence further justify the cost of the footer.

## References

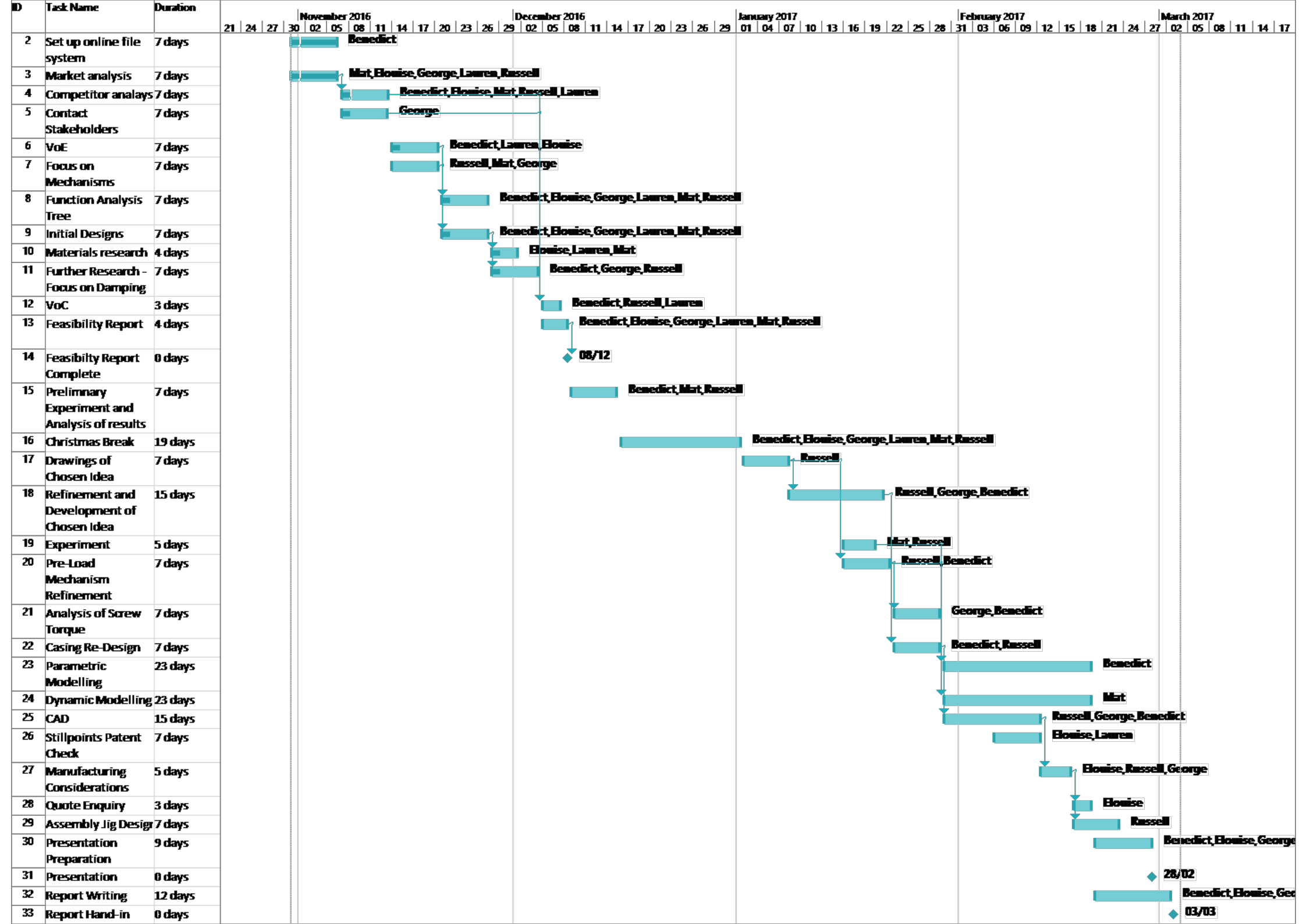
- [1] R. B. Tomer, *Getting the most out of vacuum tubes: Electron tubes valves*. Book Geek, 1960, vol. 2, p. 49.
- [2] M. A. Meyers and K. K. Chawla, *Mechanical behavior of materials*. Cambridge: Cambridge University Press, 2009, vol. 2, pp. 98–103.
- [3] R. S. Maguire, E. O. Hollands, B. A. H. Jones, L. R. Miller, G. A. Hall, and M Valladares-Hodder, “Vibration isolation and attenuation mounts”, Durham University School of Engineering and Computing Sciences, Durham, Feasibility Report, Dec. 2016.
- [4] Matweb, *Neodymium, Nd*, AMEND00 / 69, Apr. 2015.
- [5] ——, *Tungsten carbide, WC*, BCWCA / 166, Dec. 2010.
- [6] ——, *316 stainless steel, annealed bar*, MQ316J / 12797, Jun. 2014.
- [7] ——, *Aluminium 6061-t6; 6061-t651*, MA6061T6\_copy / 192050, Aug. 2016.
- [8] ——, *AISI type A2 tool steel*, MSTAA2A / 14095, Nov. 2008.
- [9] A. Blake, *What every engineer should know about threaded fasteners: Materials and design*. CRC Press, 1986, pp. 102–106.
- [10] J. Archard and W Hirst, “The wear of metals under unlubricated conditions”, in *Proceedings of the royal society of london a: Mathematical, physical and engineering sciences*, The Royal Society, vol. 236, 1956, pp. 397–410.
- [11] J. Stokes, “Man/system requirements for weightless environments”, NASA-MSFC, Tech. Rep., 1976.

- [12] D. Vokoun, M. Beleggia, L. Heller, and P. Šittner, “Magnetostatic interactions and forces between cylindrical permanent magnets”, *Journal of magnetism and magnetic materials*, vol. 321, no. 22, pp. 3758–3763, 2009.
- [13] *Magnetic pull force*, <http://www.codecogs.com/library/physics/magnetism/magnetic-pull-force.php>, [Online; accessed 1-March-2017].
- [14] G. T. Nakai, “Dynamic damping of stylus compliance/tone-arm resonance”, *Journal of the audio engineering society*, vol. 21, no. 7, pp. 555–562, 1973.
- [15] ST Microelectronics, *MEMS inertial sensor high performance 3-axis ultracompact linear accelerometer*, LIS344ALH, Oct. 2015.
- [16] *Modelling mass-spring-damper system in simulink and simscape*, [https://www.mathworks.com/examples/simscape/mw/simscape\\_product-ssc\\_mass\\_spring\\_damper\\_sl-mass-spring-damper-in-simulink-and-simscape](https://www.mathworks.com/examples/simscape/mw/simscape_product-ssc_mass_spring_damper_sl-mass-spring-damper-in-simulink-and-simscape), [Online; accessed 20-February-2017].
- [17] D. Cochrane, *Guide to stainless steel finishes*. Euro Inox, 2000.
- [18] *Stillpoints ultra 6*, <https://www.audiodesignation.co.uk/stillpoints>, [Online; accessed 20-February-2017].
- [19] P. Wakeen and L. Jacoby, *Universal vibration damper*, US Patent 6,655,668, Feb. 2003. [Online]. Available: <http://www.google.co.uk/patents/US6655668>.

## A Project Plan

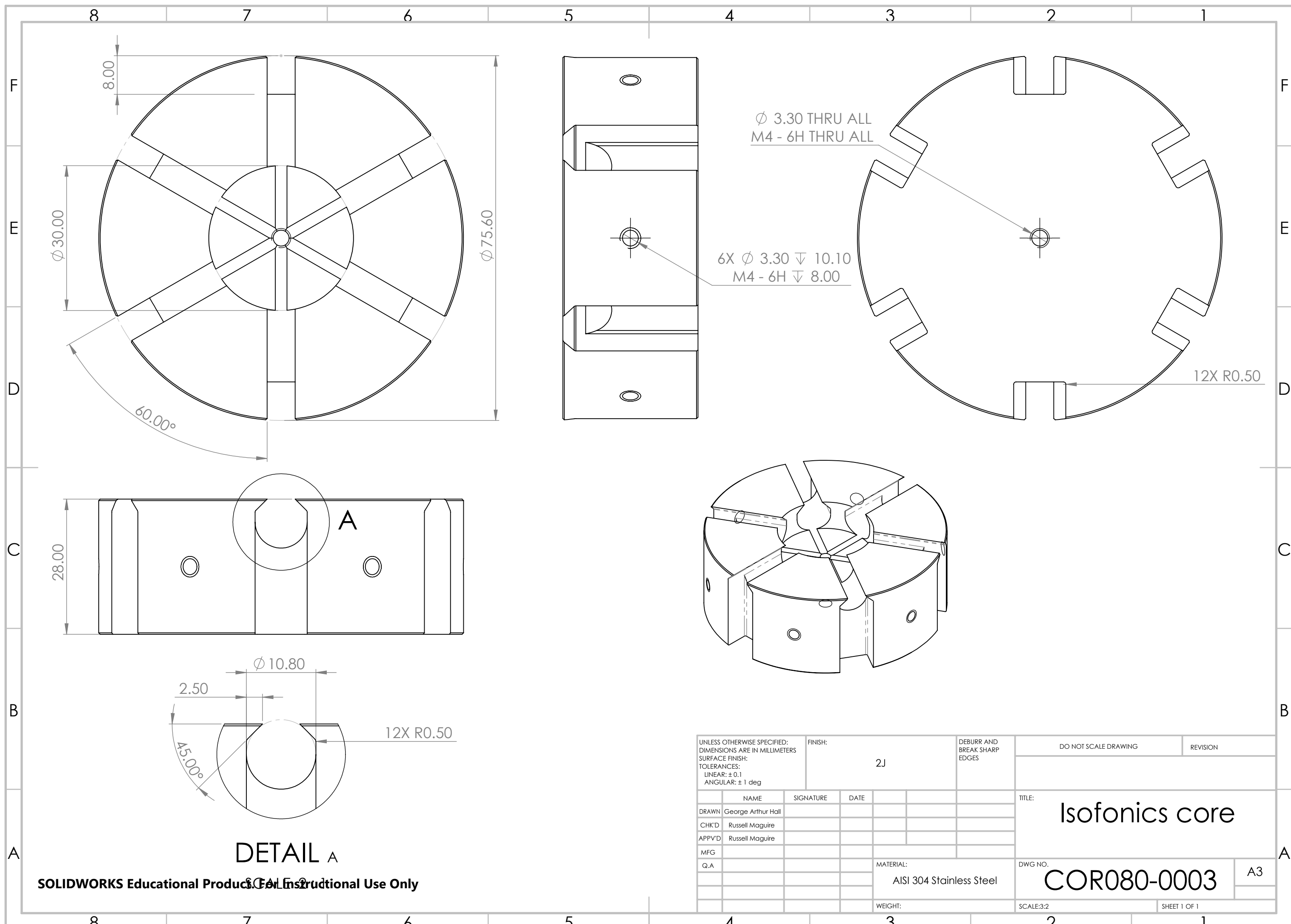
The following page details the Gantt chart for the project plan.

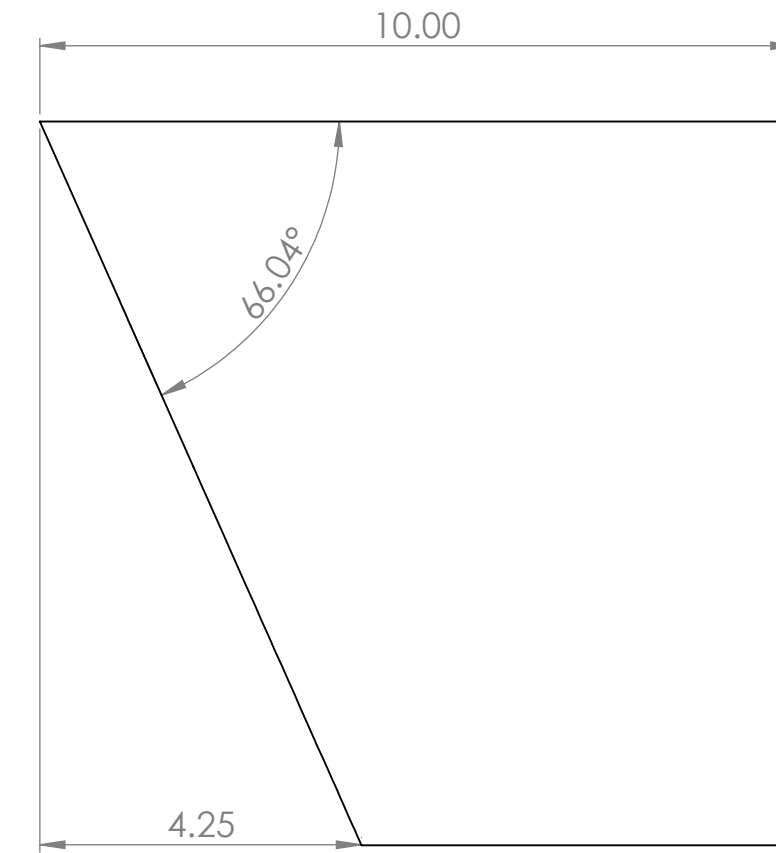
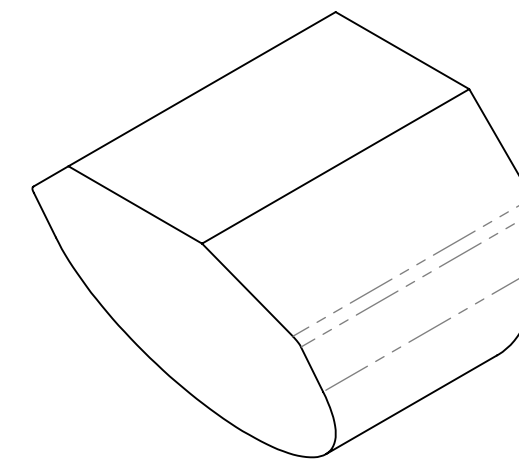
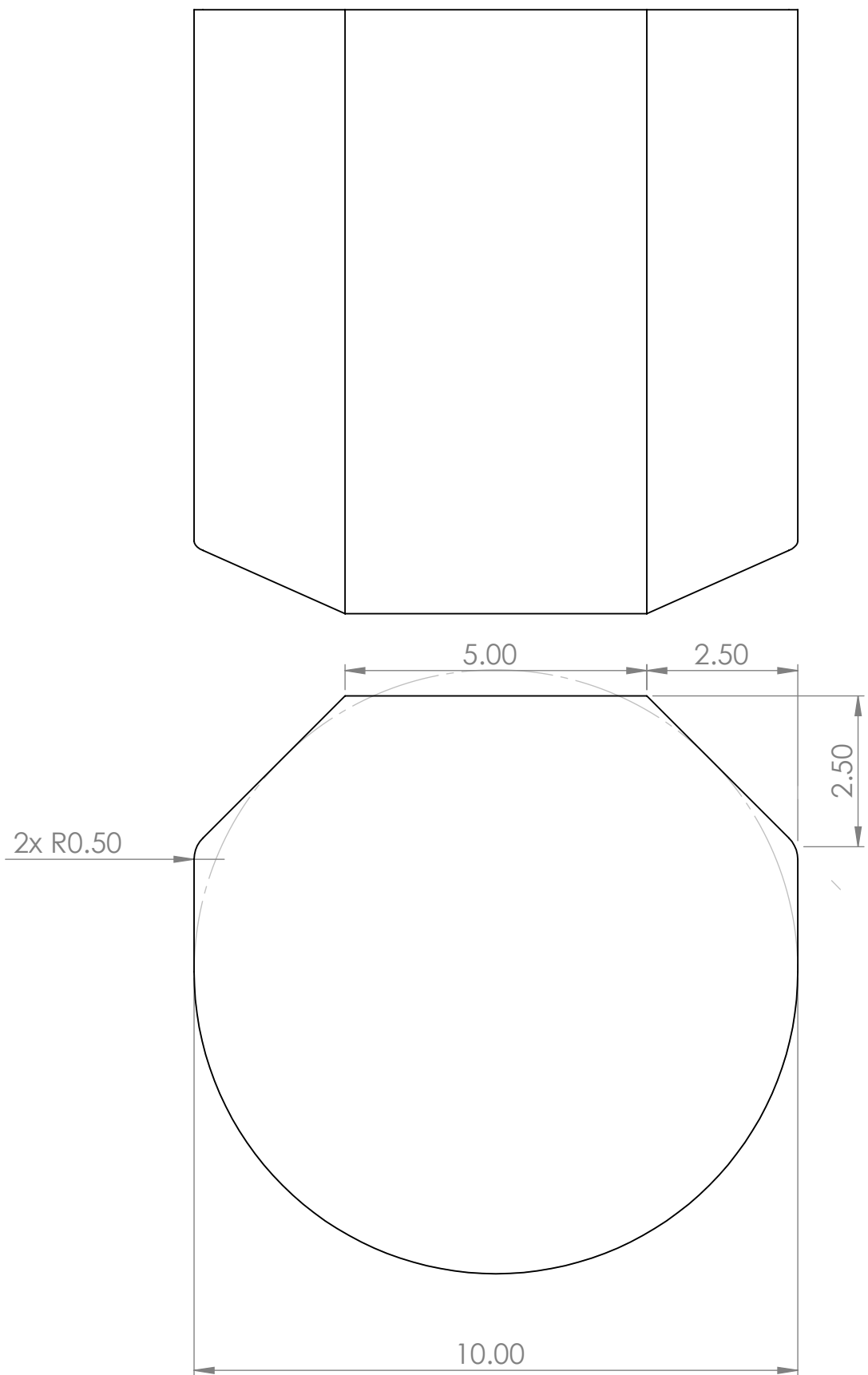
Comparing the predicted plan against the implemented plan shows many discrepancies; primarily, tasks generally took longer than expected with more than one taking place at a time. Rather than the team flowing from task to task as planned, individuals worked on a particular section for an extended period. This allowed the team to delegate tasks more effectively, ensuring that the workload was distributed evenly. Another advantage to this method was that each member of the team gained a deeper understanding in the field which they were working on, this lead to a more comprehensive analysis being performed. Although several team members were assigned to each task, they were generally split into smaller subsections and individual work was coalesced.



## B Drawings

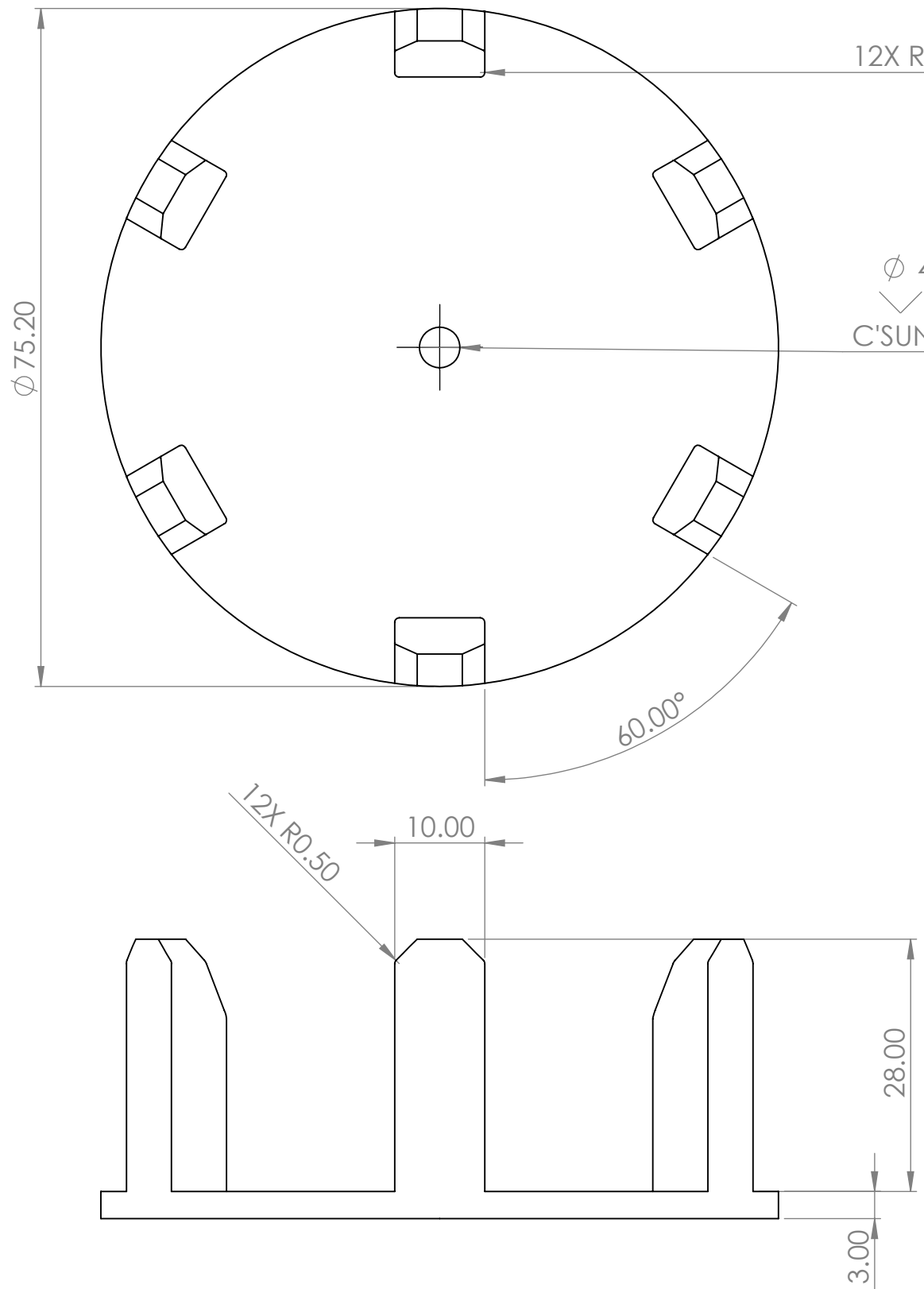
The following pages detail final drawings for the custom parts required for the footer. Also detailed are the parts required to build the assembly jig.





**SOLIDWORKS Educational Product. For Instructional Use Only**

|   |                    |                                    |            |                                    |  |          |
|---|--------------------|------------------------------------|------------|------------------------------------|--|----------|
| UNLESS OTHERWISE SPECIFIED:<br>DIMENSIONS ARE IN MILLIMETERS<br>SURFACE FINISH:<br>TOLERANCES:<br>LINEAR: ± 0.1<br>ANGULAR: ± 1 deg |                    | FINISH:<br><br>Brushed             |            | DEBURR AND<br>BREAK SHARP<br>EDGES | DO NOT SCALE DRAWING                           | REVISION |
|   |                    |                                    |            |                                    | TITLE:<br><br>Isofonics preloading<br>backstop |          |
| DRAWN   | George Arthur Hall |                                    |            |                                    |  |          |
| CHK'D   | Russell Maguire    |                                    |            |                                    |  |          |
| APPVD   | Russell Maguire    |                                    |            |                                    |  |          |
| MFG   |                    |                                    |            |                                    |  |          |
| Q.A   |                    | MATERIAL:<br><br>6061-T6 Aluminium |            | DWG NO.<br><br>PLD010-1004         | A3   |          |
|   |                    | WEIGHT:                            | SCALE:10:1 | SHEET 1 OF 1                       |  |          |



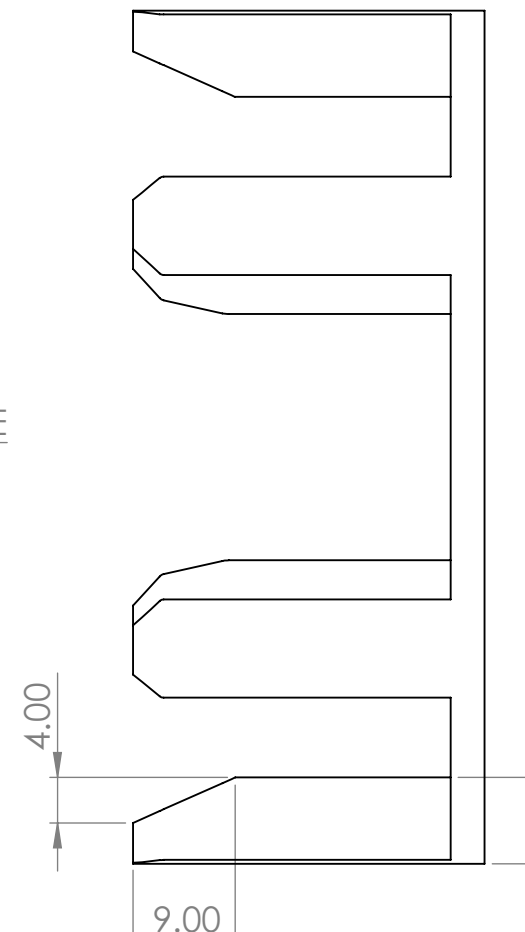
12X R0.50

$\phi$  4.50 THRU ALL  
 $\checkmark$   $\phi$  9.40 X 90°  
 C'SUNK ON FAR SIDE

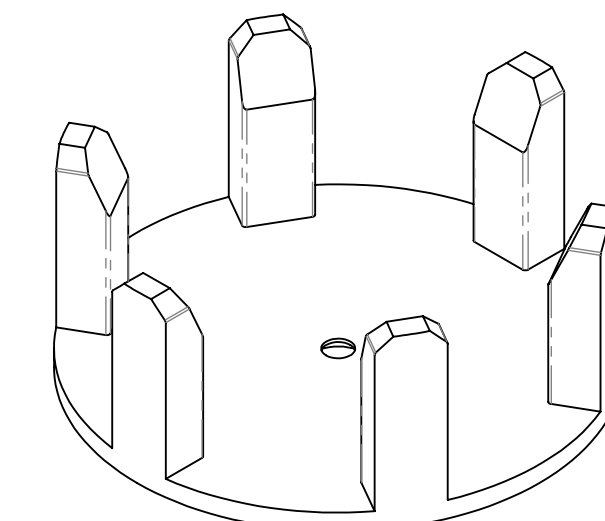
300  
28.00  
3.00

10.00  
12X R0.50

60.00°



4.00  
9.00  
7.60



UNLESS OTHERWISE SPECIFIED:  
 DIMENSIONS ARE IN MILLIMETERS  
 SURFACE FINISH:  
 TOLERANCES:  
 LINEAR: ± 0.1  
 ANGULAR: ± 1 deg

DRAWN George Arthur Hall

CHK'D Russell Maguire

APP'D Russell Maguire

MFG

Q.A.

FINISH:  
Brushed

DEBURR AND  
BREAK SHARP  
EDGES

DO NOT SCALE DRAWING

REVISION

TITLE:

Isofonics  
 preloading crown  
 PLD080-0003

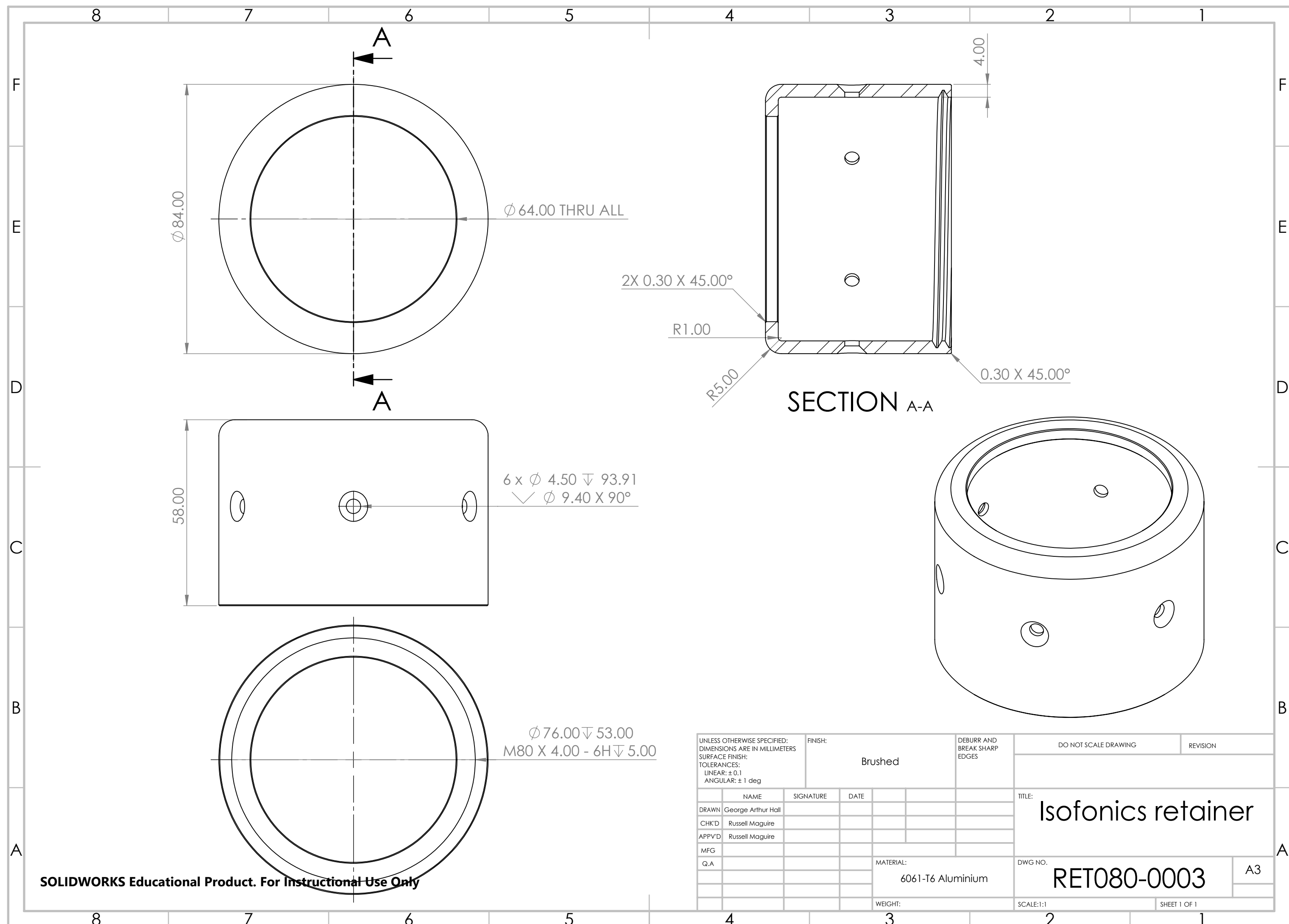
DWG NO.

6061-T6 Aluminium

SCALE: 3:2

A3

SHEET 1 OF 1



8

7

6

5

4

3

2

1

F

F

E

E

D

D

C

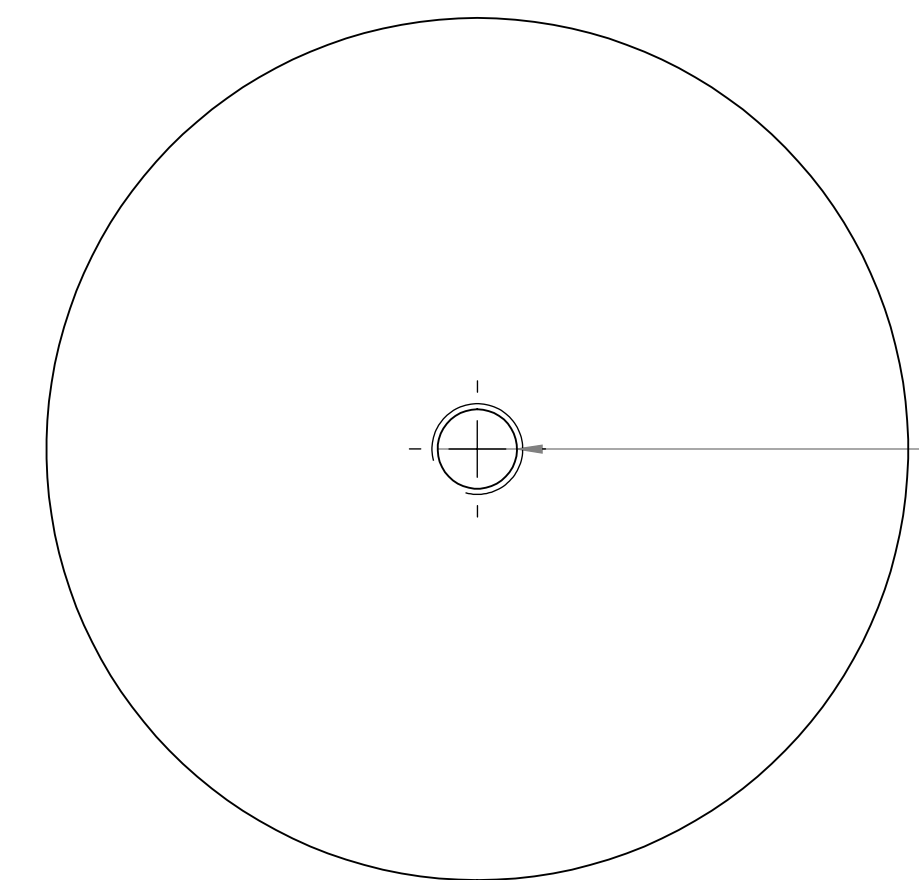
C

B

B

A

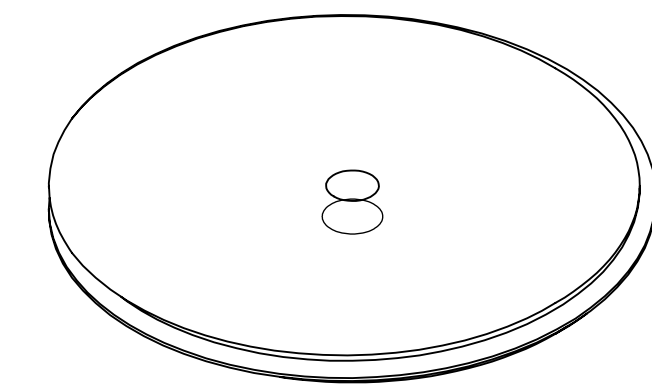
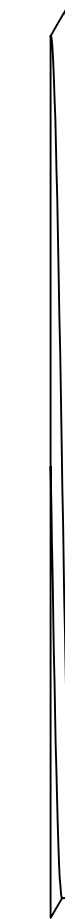
A



$\emptyset$  7.00 THRU ALL  
M8x1.0 - 6H THRU ALL

5.00

M80 X 4.00



UNLESS OTHERWISE SPECIFIED:  
DIMENSIONS ARE IN MILLIMETERS  
SURFACE FINISH:  
TOLERANCES:  
LINEAR:  $\pm 0.1$   
ANGULAR:  $\pm 1$  deg

|       | NAME               | SIGNATURE | DATE |  |
|-------|--------------------|-----------|------|--|
| DRAWN | George Arthur Hall |           |      |  |
| CHK'D | Russell Maguire    |           |      |  |
| APP'D | Russell Maguire    |           |      |  |
| MFG   |                    |           |      |  |
| Q.A.  |                    |           |      |  |

Brushed

DEBURR AND  
BREAK SHARP  
EDGES

MATERIAL:  
6061-T6 Aluminium

DO NOT SCALE DRAWING

REVISION

TITLE: Isofonics retainer bottom

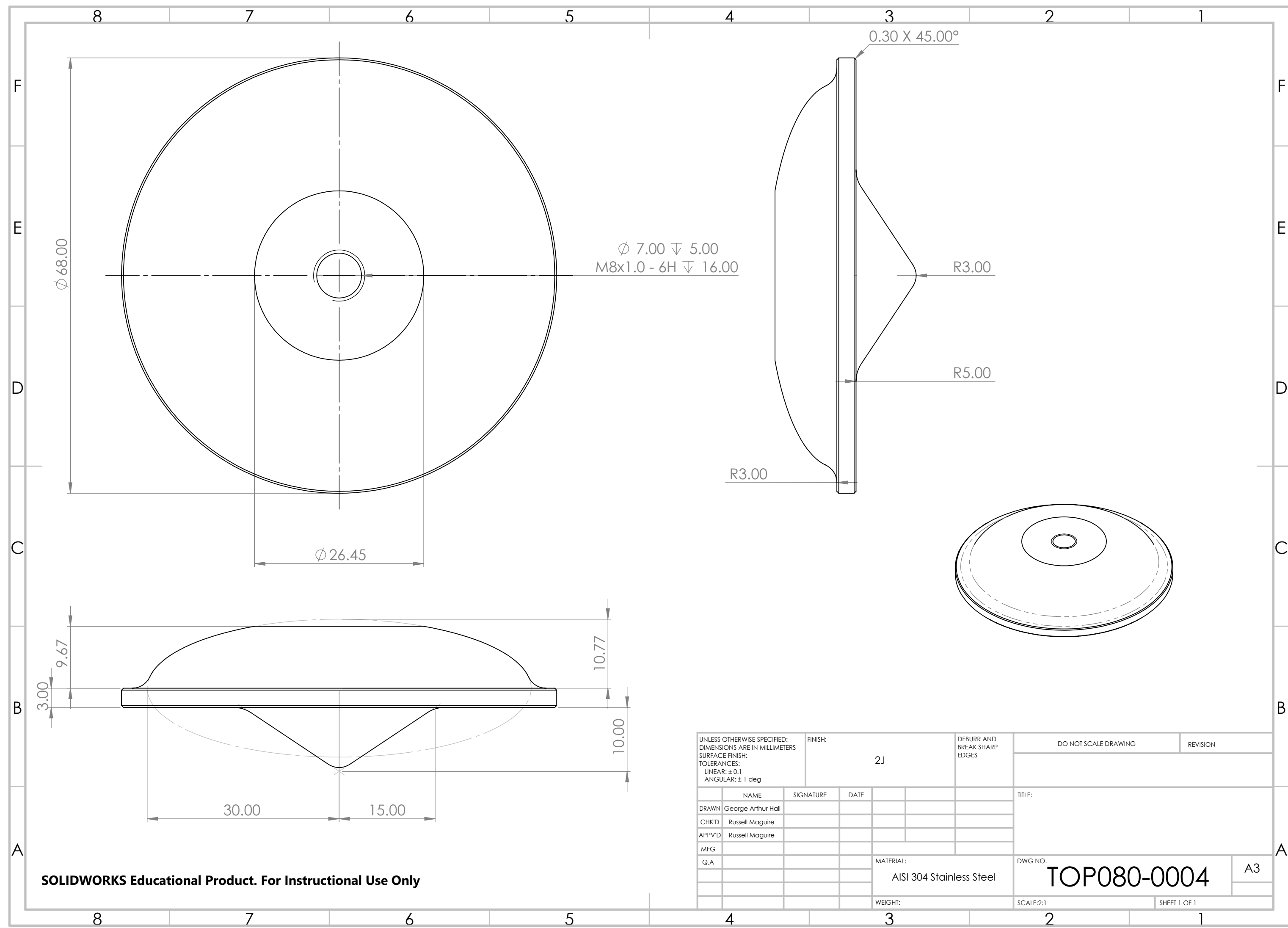
DWG NO. RET080-1002

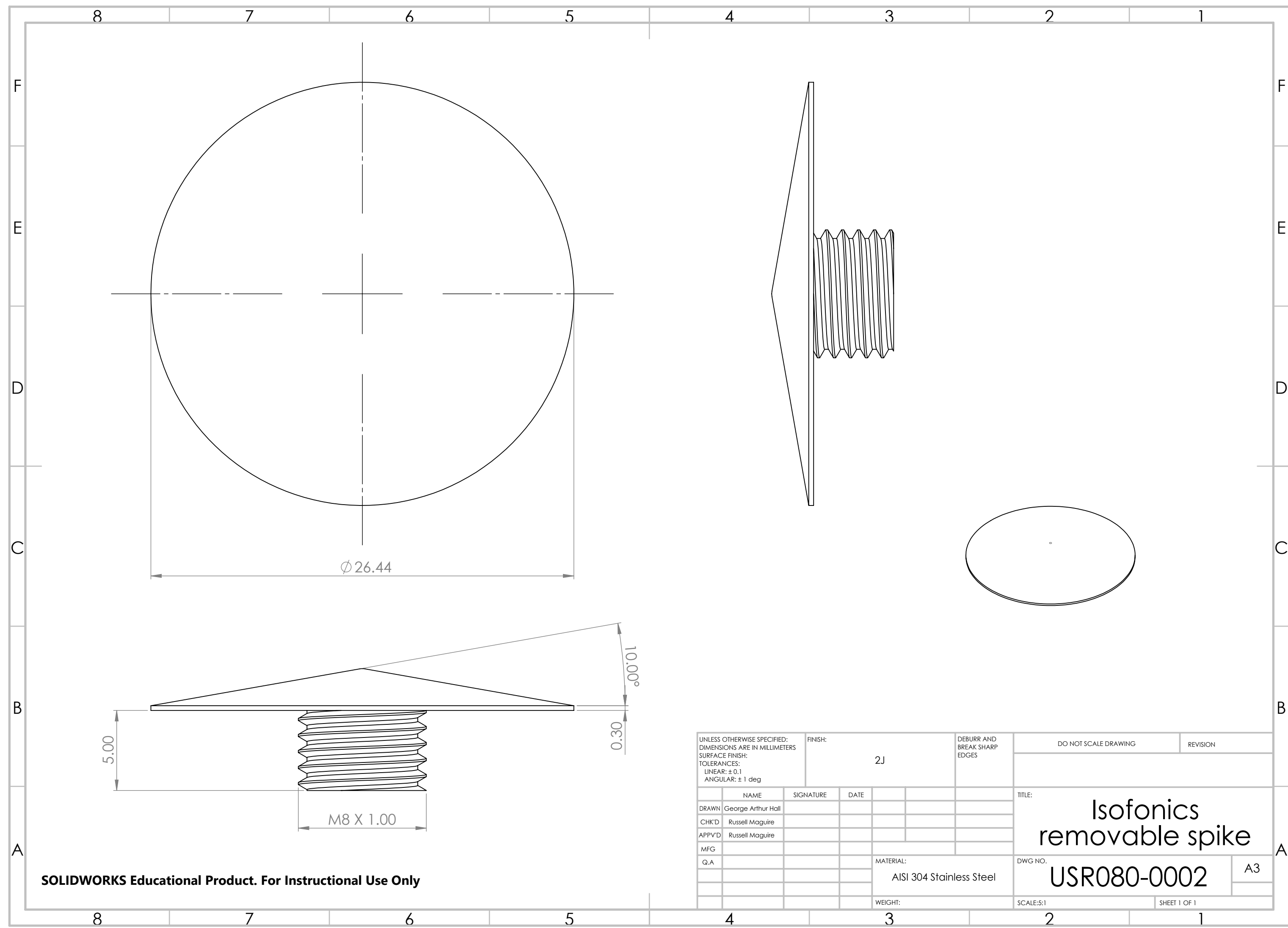
A3

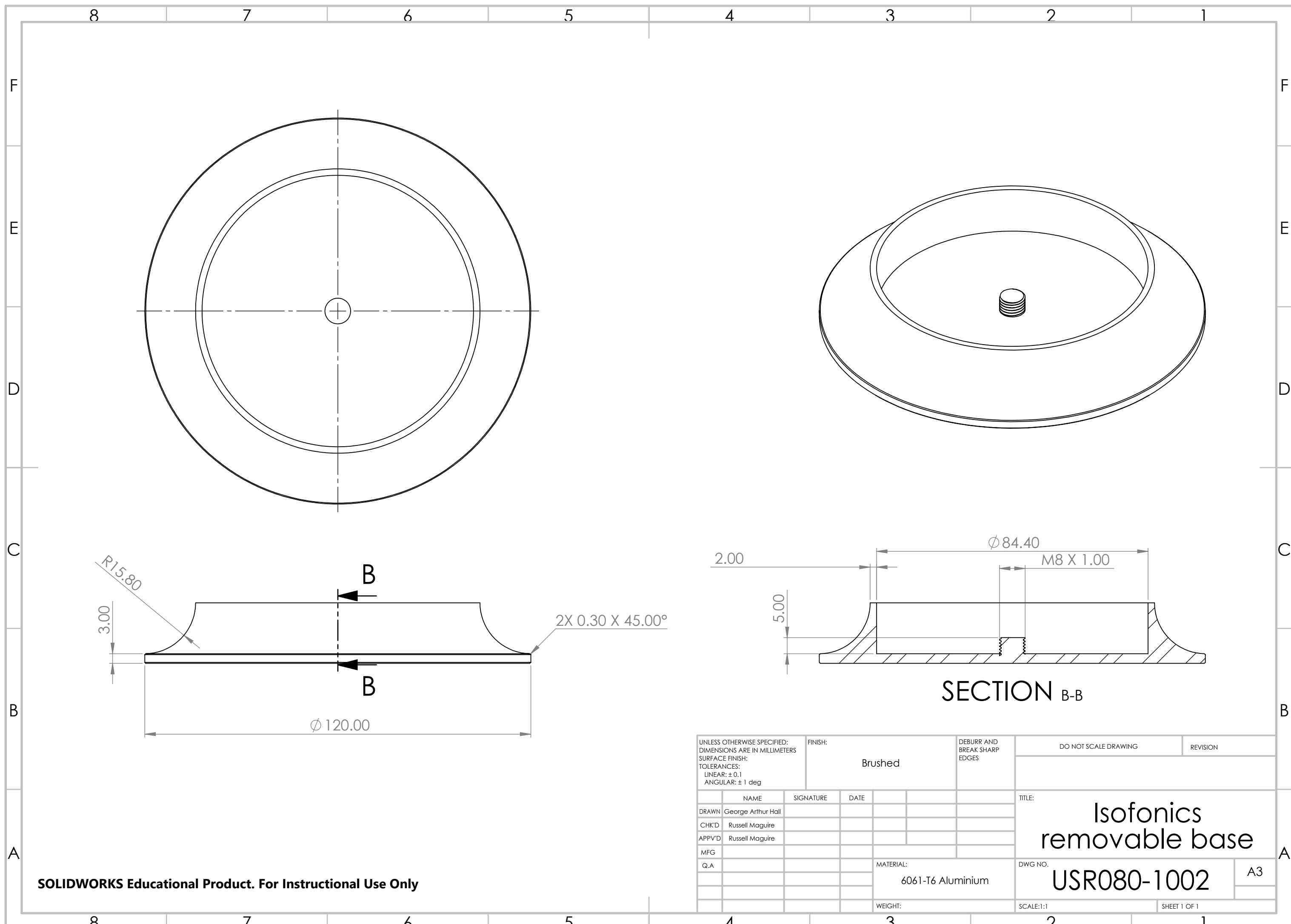
SCALE: 3:2

WEIGHT:

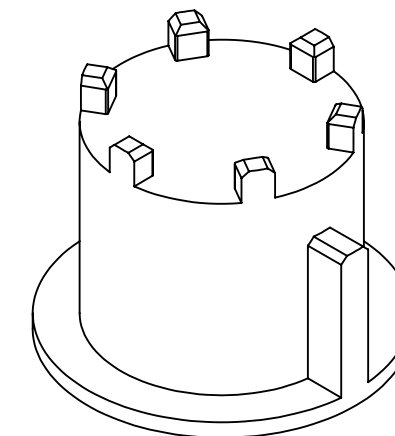
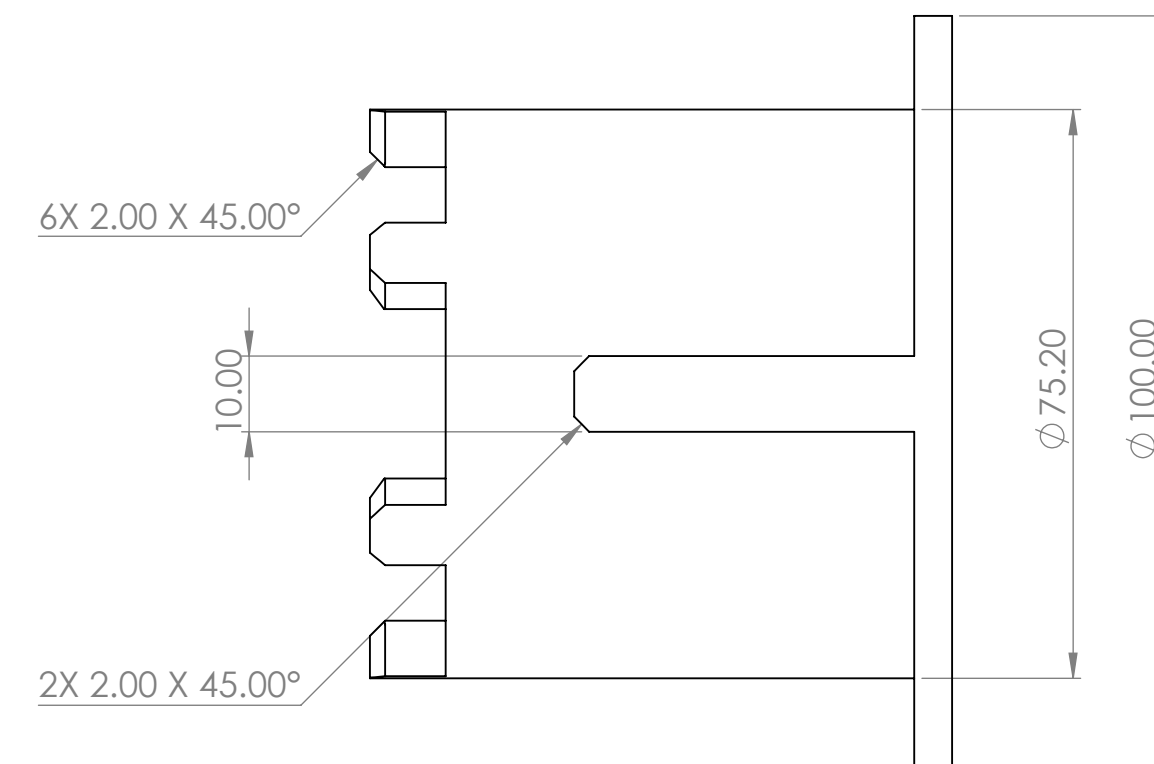
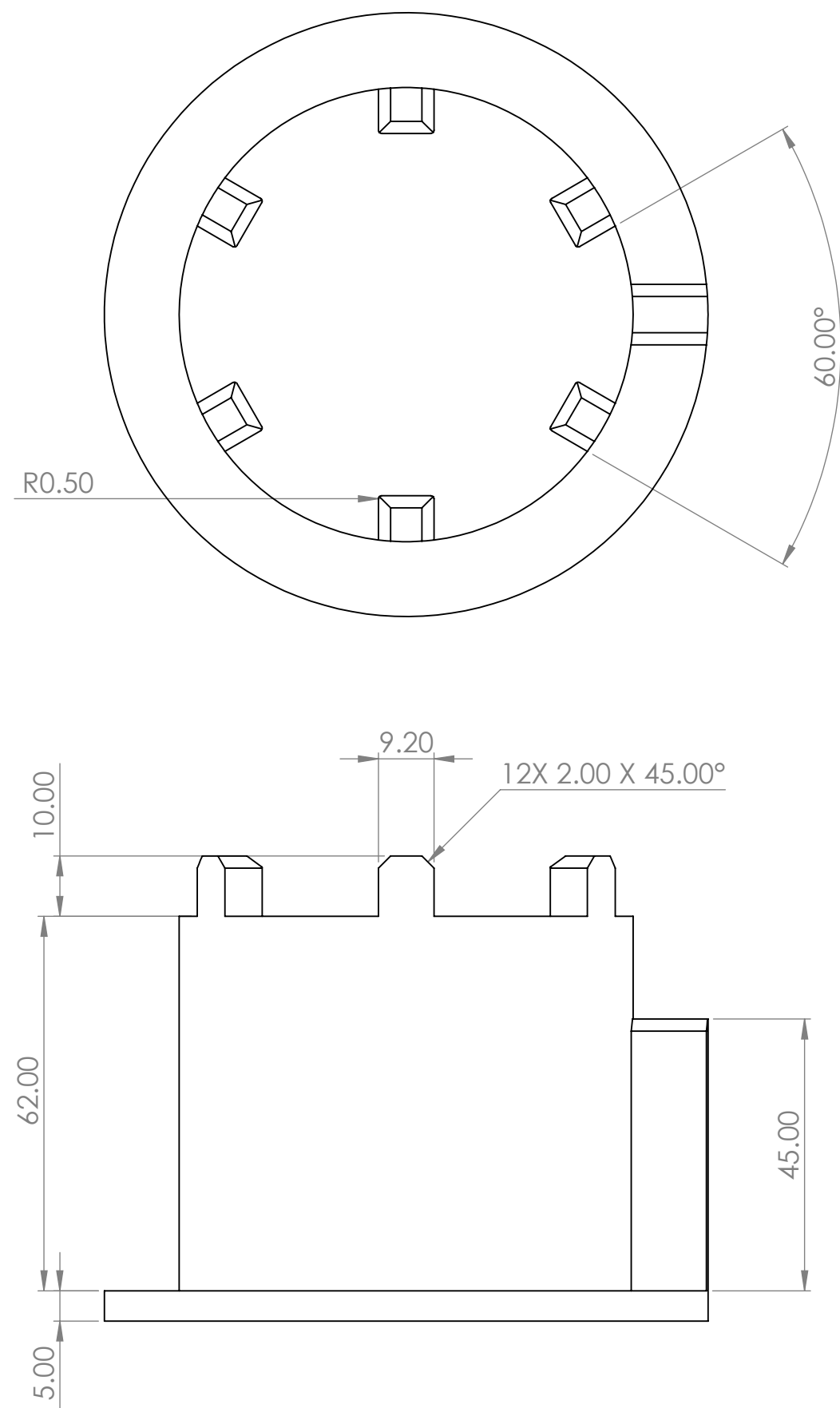
SCALE 1 OF 1





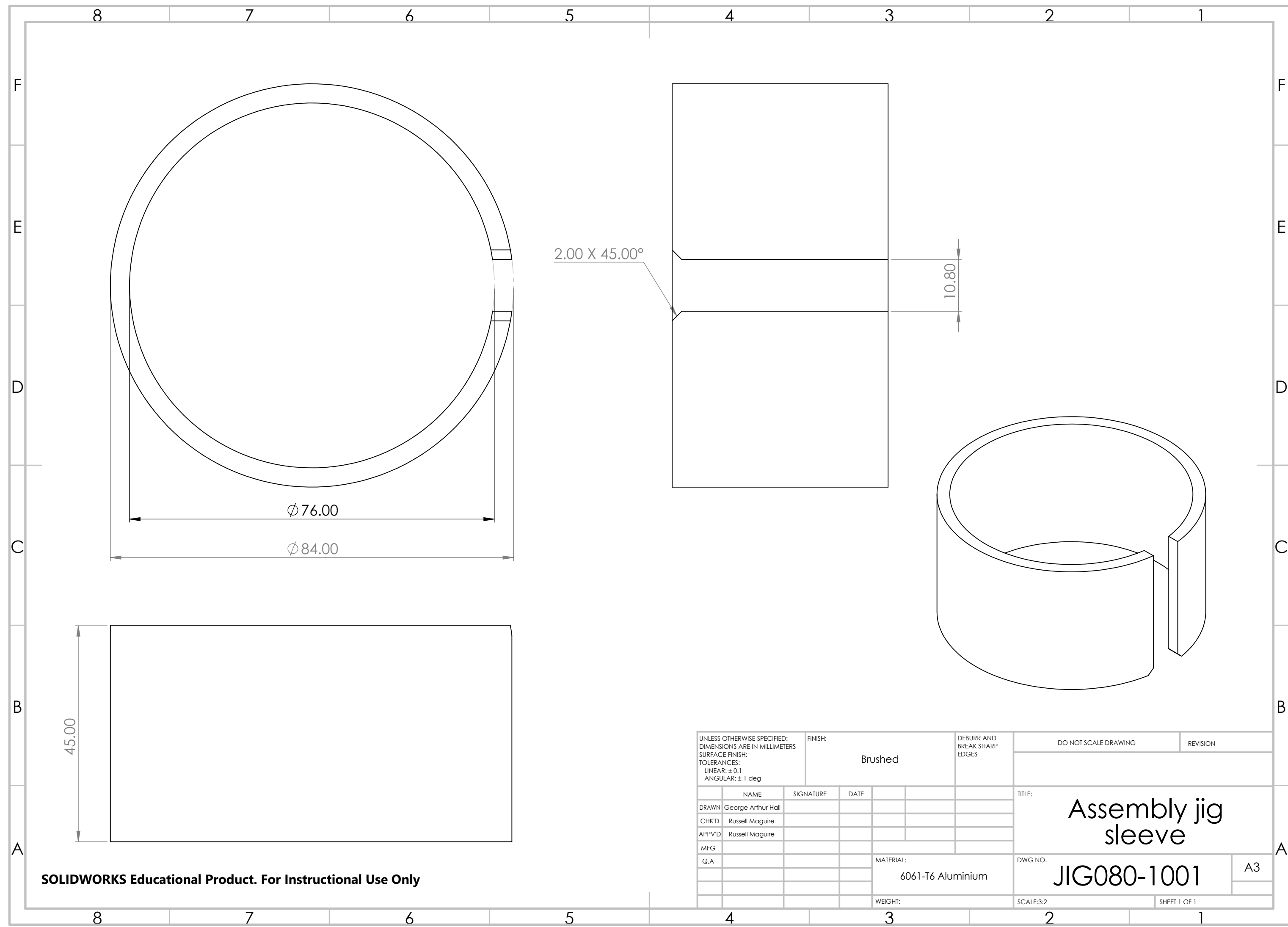


**SOLIDWORKS Educational Product. For Instructional Use Only**



**SOLIDWORKS Educational Product. For Instructional Use Only**

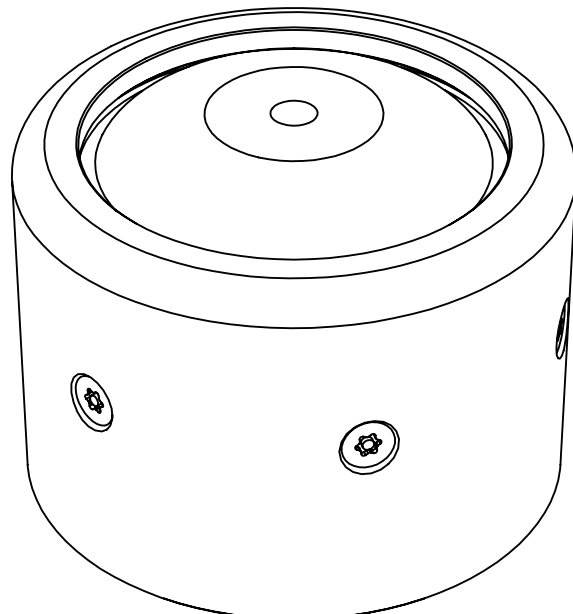
|   |                    |                        |           |                                    |                      |              |
|---|--------------------|------------------------|-----------|------------------------------------|----------------------|--------------|
| UNLESS OTHERWISE SPECIFIED:<br>DIMENSIONS ARE IN MILLIMETERS<br>SURFACE FINISH:<br>TOLERANCES:<br>LINEAR: ± 0.1<br>ANGULAR: ± 1 deg |                    | FINISH:<br><br>Brushed |           | DEBURR AND<br>BREAK SHARP<br>EDGES | DO NOT SCALE DRAWING | REVISION     |
|   | NAME               | SIGNATURE              | DATE      |                                    |                      |              |
| DRAWN   | George Arthur Hall |                        |           |                                    |                      |              |
| CHK'D   | Russell Maguire    |                        |           |                                    |                      |              |
| APP'VD  | Russell Maguire    |                        |           |                                    |                      |              |
| MFG   |                    |                        |           |                                    |                      |              |
| Q.A   |                    |                        | MATERIAL: | 6061-T6 Aluminium                  |                      | DWG NO.      |
|   |                    |                        | WEIGHT:   |                                    |                      | SCALE:1:1    |
|   |                    |                        |           |                                    |                      | SHEET 1 OF 1 |



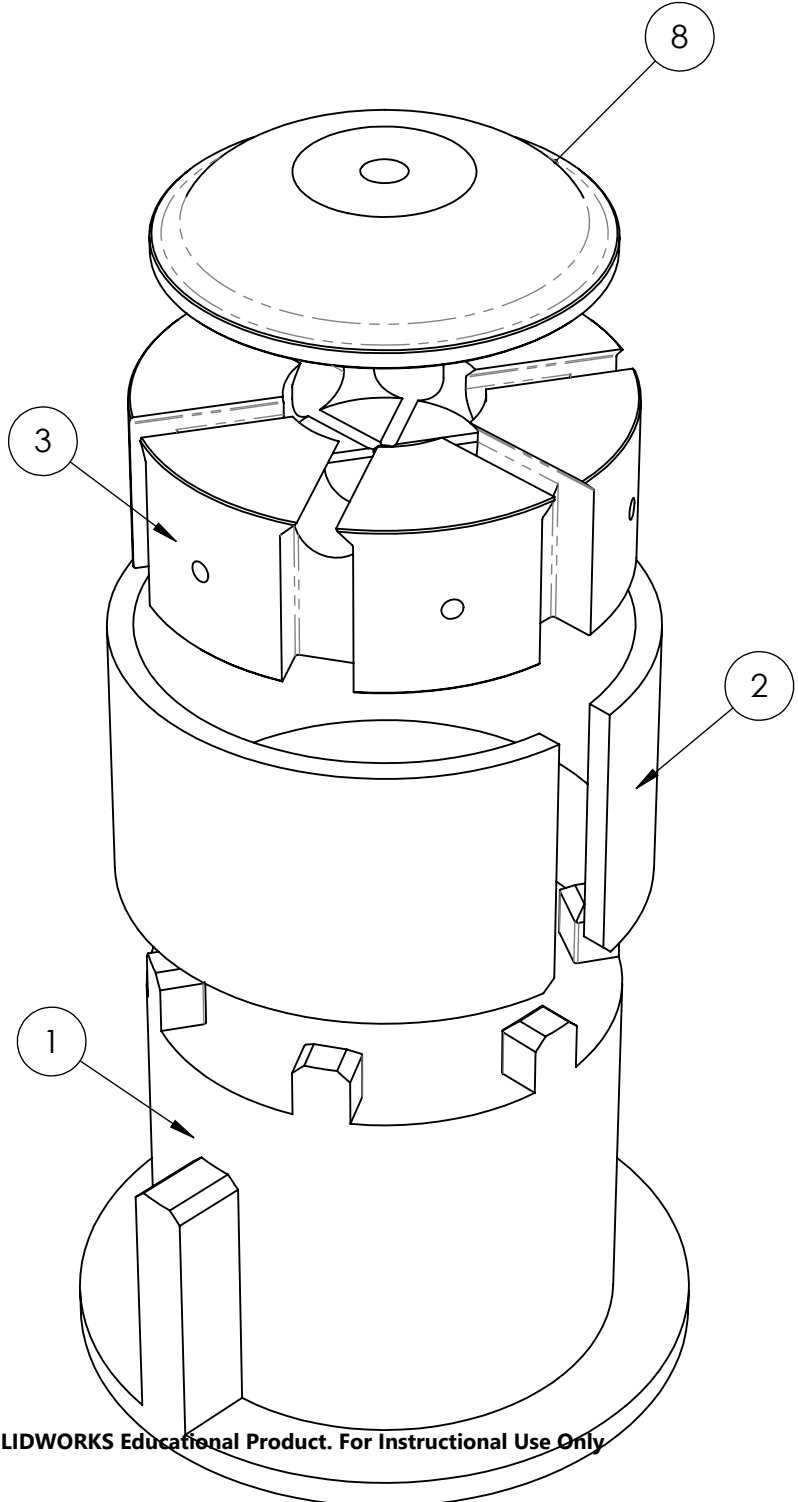
## C Assembly Instructions

The following pages detail the assembly instructions which would be a deliverable whitepaper document to the third party contractor tasked with assembling a batch of Isofonics footers.

**ISOFONICS**  
Assembly Instructions  
ISO080-INS  
R. S. Maguire

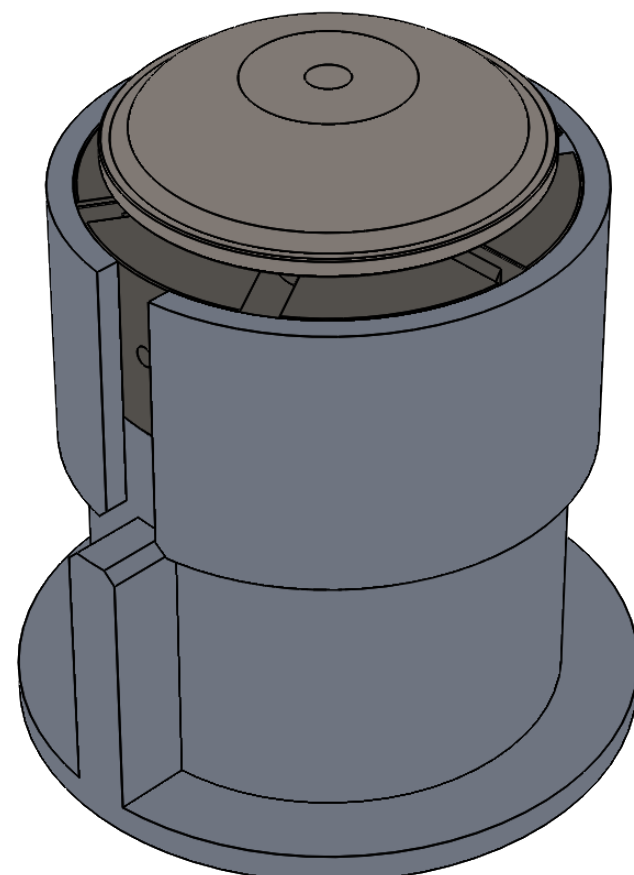


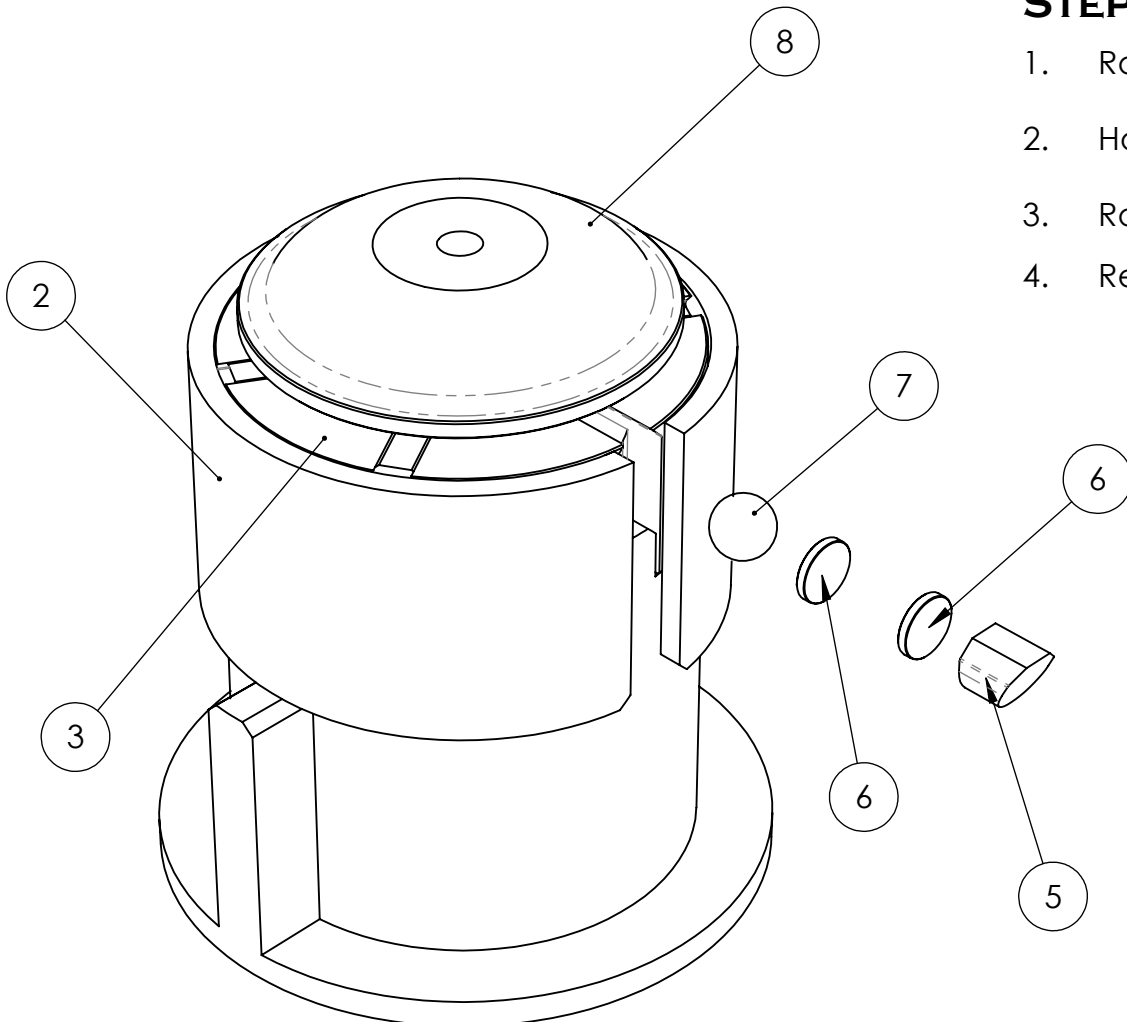
| ITEM NO. | PART NUMBER                          | DESCRIPTION   | QTY. |
|----------|--------------------------------------|---|------|
| 1        | JIG080-0001                          | Assembly jig base                                       | 1    |
| 2        | JIG080-1001                          | Assembly jig sleeve                                     | 1    |
| 3        | COR080-0003                          | Isofonics core  | 1    |
| 4        | PLD080-0003                          | Isofonics preloading crown                              | 1    |
| 5        | PLD010-1004                          | Isofonics preloading backstop                           | 6    |
| 6        | F669-N45SH-10<br>(first4magnets)     | 10 x 1.5mm neodymium magnet                             | 12   |
| 7        | 10MMTUNGSTENBAL<br>LS (VXB Bearings) | 10mm tungsten carbide ball                              | 6    |
| 8        | TOP080-0004A                         | Isofonics top piece                                     | 1    |
| 9        | RET080-0003                          | Isofonics retainer                                      | 1    |
| 10       | M4X20-CSK-ST<br>(westfieldfasteners) | Partially threaded M4 x 20mm<br>c'sunk security screw   | 6    |
| 11       | M4X20-CSK-H<br>(westfieldfasteners)  | Partially threaded M4 x 20mm<br>c'sunk hex socket screw | 1    |
| 12       | RET080-1002                          | Isofonics retainer bottom                               | 1    |



### STEP 1

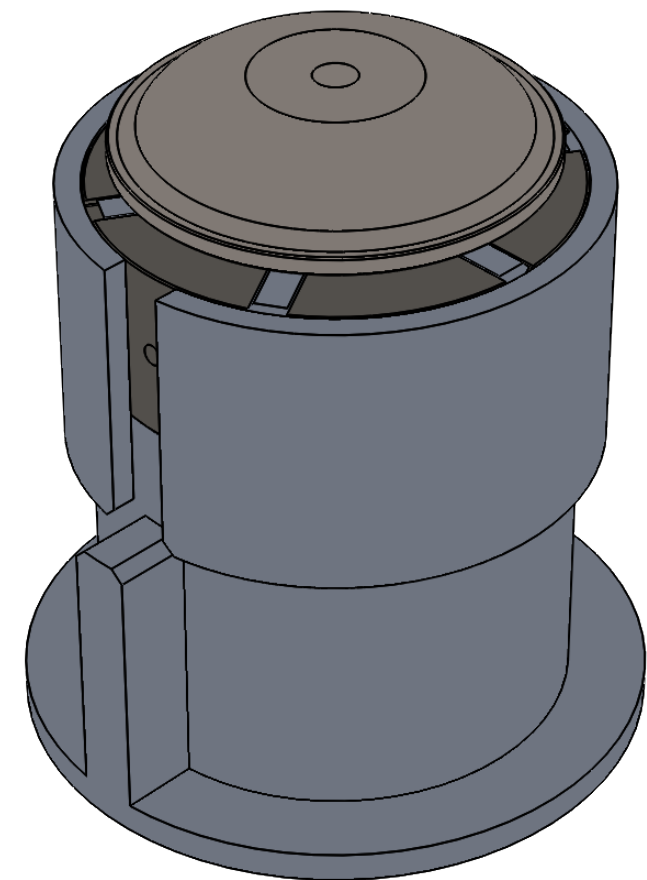
1. Slot 3 into 1
2. Slide 2 over 1
3. Place 8 ontop of 3





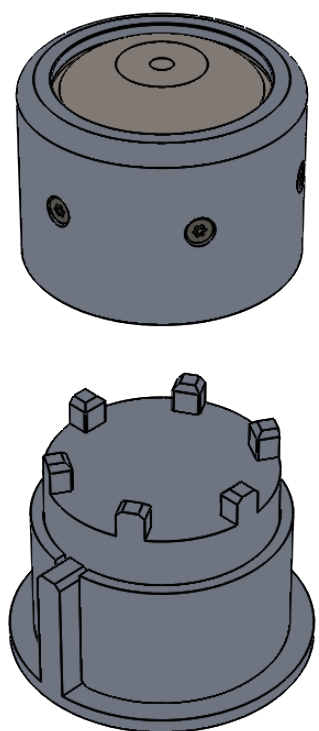
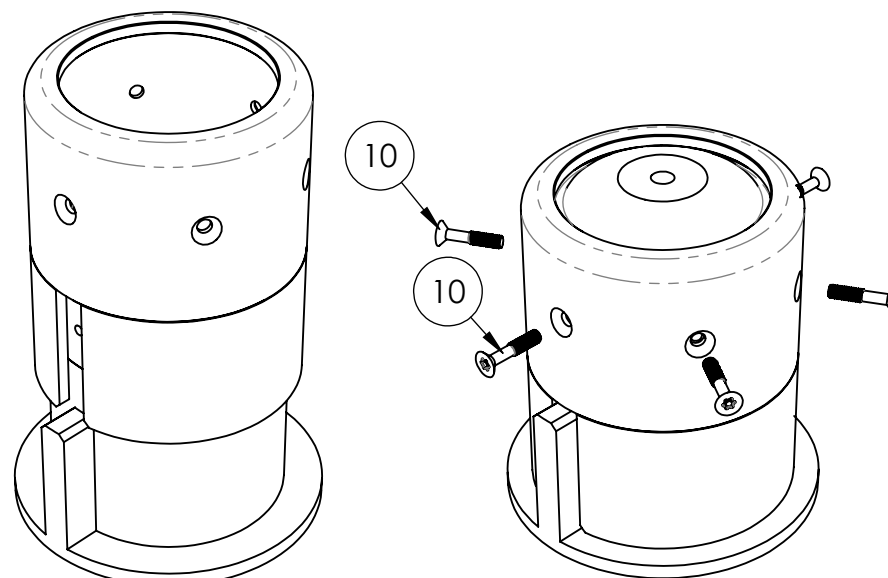
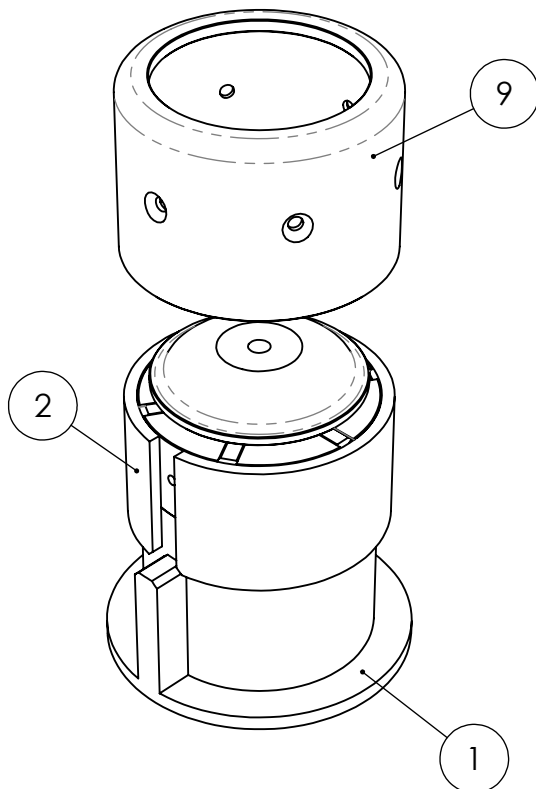
## STEP 2

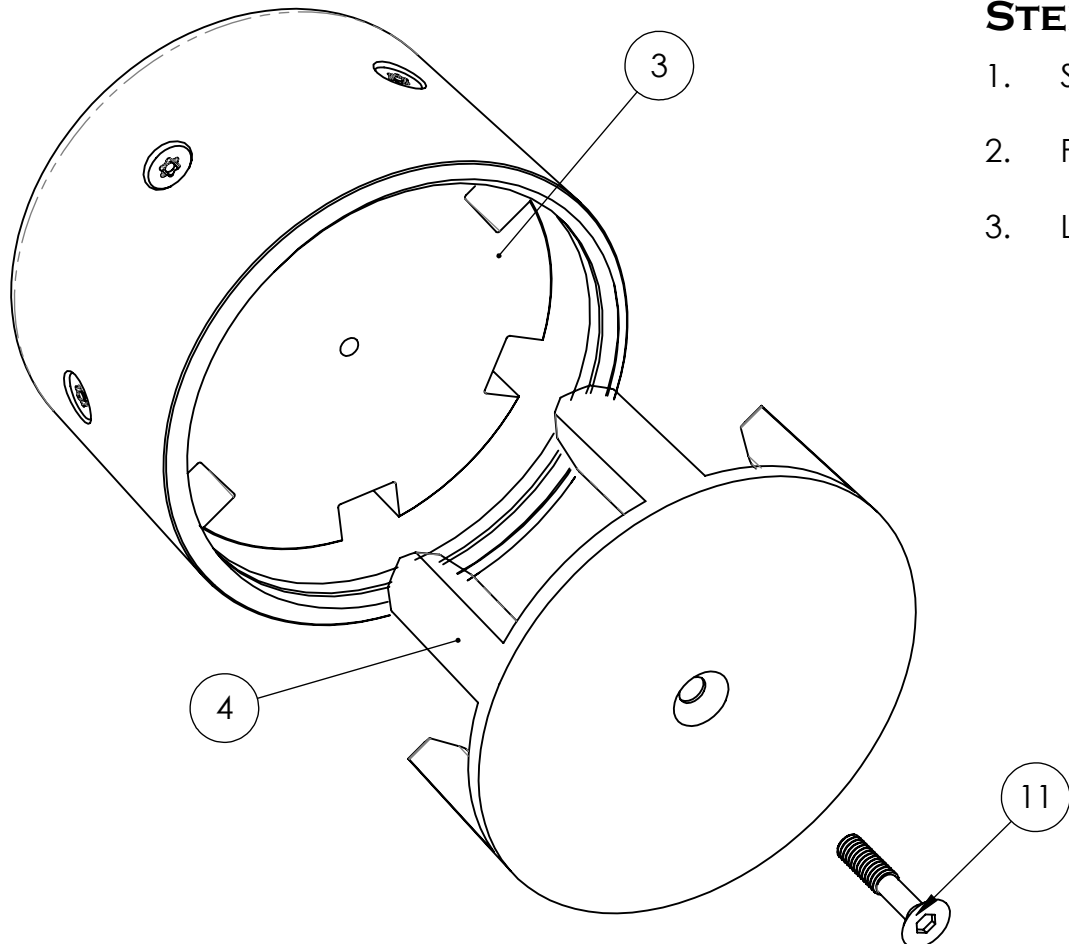
1. Rotate 2 until parallel with track in 3
2. Holding firmly onto 8, slide parts onto track
3. Rotate 2 so parts are contained
4. Repeat for all six tracks



### STEP 3

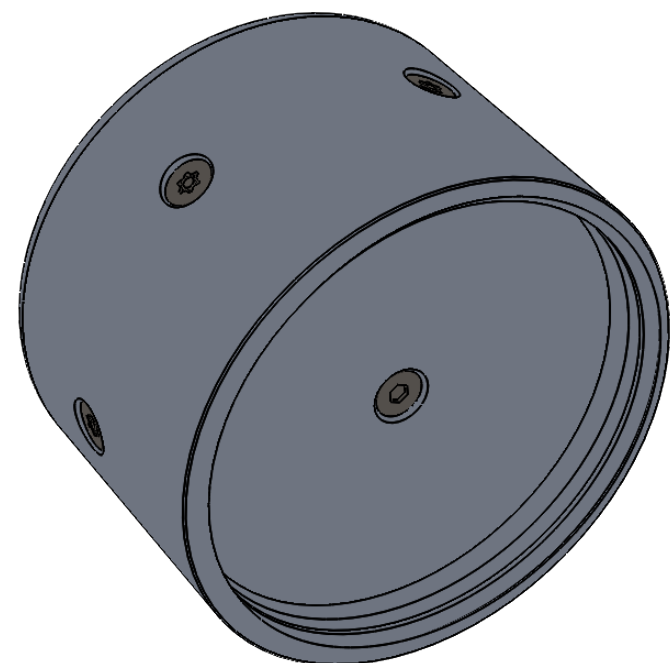
1. Rotate ② until parallel with notch in ①
2. Slide ⑨ over assembly, pushing down ②
3. Fasten ⑨ with 6x ⑩
4. Remove ① and ②





#### STEP 4

1. Slot 4 into 3
2. Fasten with 11
3. Load 11 to 0.0250 Nm



## STEP 5

1. Screw (12) into (9)

